Necrostatin-1 as a Neuroprotectant

Danuta Jantas and Władysław Lasoń

Contents

Abstract

Necrostatin-1 (Nec-1) is an inhibitor of necroptosis, a form of regulated nonapoptotic cell death pathway. It acts via allosteric blockade of receptor-interacting protein 1 (RIP1) kinase, thereby preventing the formation of the necrosome complex and execution of necroptotic program. Apart from serving a crucial physiological role during development and adulthood, necroptosis has been implicated in the pathogenesis of various human pathologies including acute and chronic neurodegenerative conditions. This chapter summarizes experimental data on neuroprotective effects of Nec-1 and current views on its molecular mechanisms of action. It also highlights advantages and limitations of Nec-1 as a potential neuroprotectant. Nec-1 showed marked neuroprotective properties in a wide range of in vivo experimental models of

D. Jantas (✉) · W. Lasoń
Maj Institute of Pharmacology Polish Academy of Sciences, Department of Experimental Neuroendocrinology, Krakow, Poland
e-mail: jantas@if-pan.krakow.pl; lason@if-pan.krakow.pl

R. M. Kostrzewa (ed.), *Handbook of Neurotoxicity*,
https://doi.org/10.1007/978-3-031-15080-7_210

brain ischemia, neonatal hypoxia-ischemia, retinal ischemia, subarachnoid hemorrhage, traumatic brain and spinal cord injuries, neuropathies, and some neurodegenerative diseases. However, as a candidate for a clinically useful neuroprotectant, Nec-1 shows also some shortcomings. Its solubility in water is limited and its half-time after systemic administration is relatively short. Nevertheless, Nec-1 proved to be a highly valuable tool in studying the relationships between various cell death pathways enabling researchers to get more insight into severe CNS pathologies, and in this way this compound may contribute to further development of the long-desired clinically approved neuroprotectant.

Keywords

Necroptosis · RIP1 · RIP3 · MLKL · Necrostatins · Stroke · CNS injury · Neurodegenerative diseases

Abbreviations

6-OHDA	*6-hydroxydopamine*
AD	Alzhemier's disease
AIF	Apoptosis inducing factor
ALS	Amyotrophic lateral sclerosis
CNS	Central nervous system
DRP1	Dynamin-related protein 1
GSH	Glutathione
HD	Huntington's disease
I/R	Ischemia/Reperfusion
ICH	Intracerebral hemorrhage
IDO	Indoleamine 2,3-dioxygenase
MCAO	Middle cerebral artery occlusion
MLKL	Mixed lineage kinase like protein
MPTP	*1-methyl-4-phenyl-1,2,3,6-tetrahydropyridine*
Nec-1 s	Necrostatin-1 stable, *5-((7-chloro-1H-indol-3-yl)mevthyl)-3-methyl-2,4-imidazolidinedione*
Nec-1	Necrostatin-1, *5-(1H-Indol-3-ylmethyl)-(2-thio-3-methyl) hydantoin, methyl-thiohydantoin-tryptophan*
Nec-1i	Necrostatin-1 inactive, *5-(Indol-3-ylmethyl)-2-thiohydantoin*
NHI	Neonatal hypoxia-ischemia
PD	Parkinson's disease
RIP1	Receptor-interacting serine/threonine-protein kinase 1
RIP3	Receptor-interacting serine/threonine-protein kinase 3
ROS	Reactive oxygen species
SAH	Subarachnoid hemorrhage
SCI	Spinal cord injury
SNpc	Substantia nigra pars compacta
TBI	Traumatic brain injury
TNFα	Tumor necrosis factor alpha

1 Introduction

Neurodegenerative diseases and stroke are considered worldwide one of the most important medical and economic problems in aging society. There is a firm consensus that understanding of molecular mechanisms of neuronal death is the rational way for designing clinically efficient neuroprotective agent(s). The key role of oxidative stress in acute and chronic brain damage has been firmly established. In the aging brain there is overproduction of reactive oxygen species (ROS) in conjunction with a reduction in the antioxidant defense. The brain is particularly vulnerable to oxidative stress because of its high oxygen consumption. The brain consumes about 20% of the body's total oxygen due to its metabolic activity and high need for ATP. The brain is also rich in fatty acids which are prone to oxidative damage and has relatively poor antioxidant systems. Moreover, presence of free iron and other transition metals could also facilitate neurodegeneration in particular brain regions. The most common pathomechanism of neuronal damage involves excitatory amino acid–driven excitotoxicity, and dysregulation in calcium homeostasis, which are followed by perturbations in mitochondria function, activation of proteolitic enzymes, increased production of deleterious ROS, and decreased cell defense system. Cytoskeletal disruptions, protein aggregations, deficiency of neurotrophic factors, and inflammation also occur in neurodegenerative disorders. Further remarkable progress in biomedical sciences revealed several forms of cellular death with various morphological and biochemical characteristics, which may be roughly classified as unprogrammed and programmed cell deaths. Of them necrosis is described as an unprogrammed passive process triggered by disruption of normal ion fluxes and cell death begins within minutes of injury. Its main features are mitochondrial damage with rapid energy loss, swelling and vacuolation of cell body, rupture and dissolution of nucleus, and cell lysis, with inflammation injuring adjacent tissue. Identified so far programmed cell death forms include apoptosis, necroptosis, autophagy-dependent cell death, parthanatos, pyroptosis, and ferroptosis (Conrad et al. 2016, Fan et al. 2017). Apoptosis is an active process of programmed cell destruction associated with changes in gene expression and protein synthesis occurring hours to days after injury. It is characterized by condensation and fragmentation of nuclear chromatin (DNA laddering), compaction and shrinking of cell body, the loss of phospholipid asymmetry, and budding of apoptotic bodies and phagocytosis, without inflammation or damage to surrounding tissue. Besides its involvement in pathological processes, this form of cell death is also essential for proper embryologic, pre- and postnatal development. Autophagy-dependent cell death helps to maintain cell homeostasis via removing unnecessary or dysfunctional components and delivering them from cytoplasm to lysosomes for degradation. The cells which undergo autophagy show presence of cytoplasmatic vacuoles and there is lack of chromatin condensation. Parthanatos refers to a programmed cell death pathway triggered by excessive activation of poly (ADP-ribose) polymerase 1 (PARP1) and subsequent lethal depletion of nuclear NAD+. Ferroptosis is an iron-dependent form of regulated cell death associated with ROS accumulation and lipid peroxidation. Ferroptosis has been implicated in pathogenesis of cancer and

neurodegenerative diseases. Since it is closely associated with oxidative stress, it can be prevented by inhibitors of lipid peroxidation, lipophilic antioxidants, and iron chelators (Conrad et al. 2016, Fan et al. 2017). Necroptosis (or necroptotic cell death) is the most widely studied form of nonapoptotic programmed cell death pathway characterized by necrotic cell morphological features, like the loss of plasma membrane integrity, swelling of cellular organelles, and lack of typical nuclear fragmentation (Vandenabeele et al. 2010). Apart from serving an important physiological role during development and adulthood (especially in the regulation of the immune system and inflammatory response), necroptosis has been reported to occur during acute injuries of various organs (brain, heart, lung, kidney, liver, intestine, and pancreas) suggesting that its inhibition can constitute a possible therapeutic intervention (Cao & Mu, 2020; Zhao et al. 2015). Moreover, together with other programmed forms of cell death, like apoptosis or autophagy, necroptosis has been associated with the pathogenesis of various neurodegenerative diseases (e.g., Alzhemier's disease [AD], Parkinson's disease [PD], amyotrophic lateral sclerosis [ALS], and Huntington's disease [HD]) (Cao & Mu, 2020; Zhang et al. 2017). Since the aim of this chapter is to describe neuroprotective effects of the first-generation necroptosis inhibitor, necrostatin-1 (Nec-1), only some basic information on the mechanisms of necroptotic cell death pathway will be given just to enable a proper understanding of action of necroptosis-targeted compounds.

Necroptotic cell death is a caspase-independent process whose key players are two members of receptor-interacting serine/threonine-protein kinase (RIP) family, RIP1 and RIP3 (known also as RIPK1 and RIPK3). The molecular mechanisms and cellular signaling pathways involved in necroptosis are quite complex and some steps can be shared with other types of programmed cell death pathways (e.g., extracellular apoptosis) which are often regulated in a context- and cell-type-dependent manner (Vandenabeele et al. 2010, Vanden Berghe et al. 2015, Zhang et al. 2017, Zhao et al. 2015). One of the most widely investigated triggers of necroptosis is TNFα (tumor necrosis factor alpha) and its receptor TNFR1 which together initiate this cell death pathway (Fig. 1) in various cell types under conditions of deficient or blocked caspase-8 activity (usually achieved by the use of FADD-deficient cells or by pretreatment with pan-caspase inhibitor, z-VAD-fmk) (Degterev et al. 2005). The first step in this process involves autophosphorylation of RIP1 which subsequently phosphorylates RIP3 and physically interacts with the enzyme forming a supramolecular complex called necrosome (Vandenabeele et al. 2010). Next, the activated RIP3 phosphorylates mixed lineage kinase-like protein (MLKL), enabling the formation of MLKL oligomers that translocate to the plasma membrane and cause its permeabilization. The latter process promotes the release of DAMPs (Damage Associated Molecular Patterns) such as HMGB1 (high-mobility group box 1 protein) or mitochondrial DNA which under in vivo conditions can induce immune response and inflammation (Conrad et al. 2016, Vandenabeele et al. 2010, Zhao et al., 2015). Apart from TNFR also other death receptors, like Fas or TRAIL (TNF-related apoptosis-inducing ligand), have been reported in various in vitro studies to activate necroptosis under conditions of caspase deficiency (Vandenabeele et al. 2010). Moreover, among other potential inducers of necroptotic cell death, lipopolysaccharide (LPS), toll-like receptors

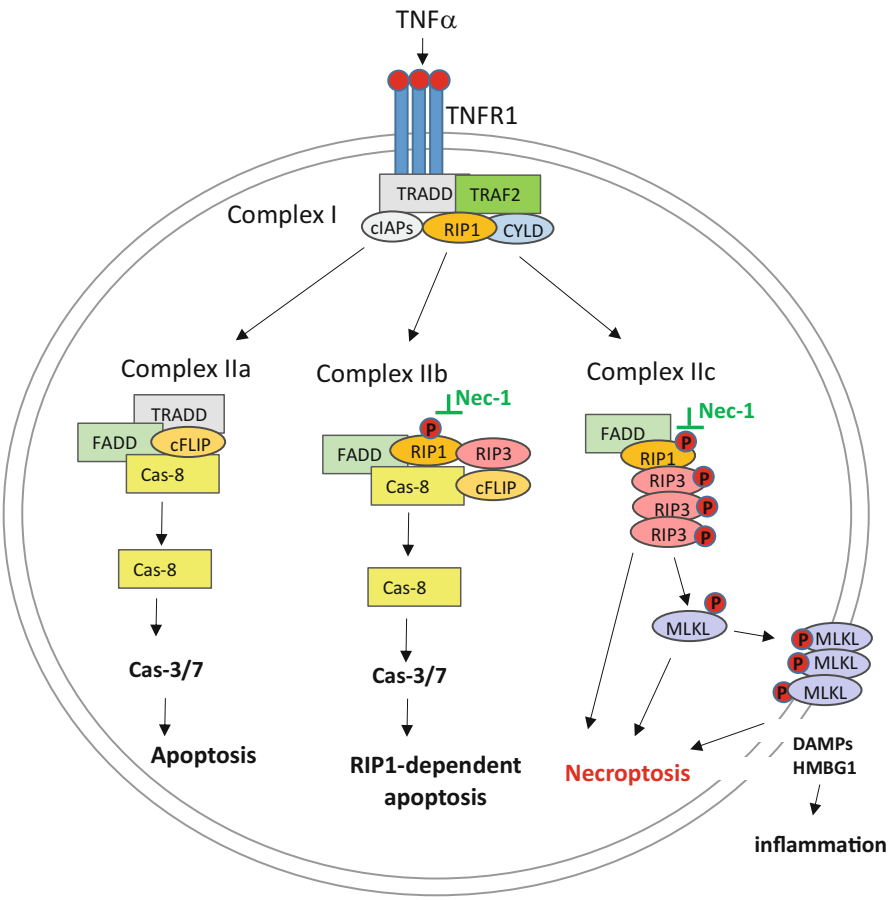

Fig. 1 Mechanisms of TNFα-induced cell death. Binding of TNFα to its receptor (TNFR1) triggers the assembly of complex I: TNFR1, TRADD (*TNFR1-associated death domain*), RIP1, TRAF2 (*TNFR-associated factor 2*), cIAPs (*cellular inhibitor of apoptosis proteins*) and CYLD (*cylindromatosis*). Under translational inhibition, TNFα stimulates the formation of a cytosolic complex IIa in which RIP1 disappears, whereas TRADD and FADD (*FAS-associated death domain*) interact in the presence of cFLIP (*cellular FLICE-like inhibitory protein*) and lead to the activation of caspase 8 (cas-8) and effector caspases (caspase 3 and caspase 7, Cas-3/7) and apoptosis. Under cIAPs inhibition complex IIb is formed (RIP1, RIP3, FADD and caspase 8) which induces RIP1-dependent apoptosis. Under conditions of caspase-8 inhibition or FADD deficiency, complex IIc (*necrosome*) is formed *via* association of RIP1 and RIP3 followed by a series of auto-and transphosphorylation of RIP1 and RIP3. Activated RIP3 phosphorylates and recruits mixed lineage kinase domain-like protein (MLKL) leading to the necroptosis. Phosphorylated MLKL translocates to the plasma membrane leading to pore formation with the release of DAMPs (*damage-associated molecular patterns*) such as HMGB1 (*high-mobility group box 1*) which induce inflammatory processes.

(TLRs), bacteria and viruses, oxidative and genotoxic stress, excitotoxicity, and calcium overload have been listed. However, the detailed mechanisms of their contribution to the activation of this cell death route still remain obscure (Conrad et al. 2016).

Some data from studies with transgenic models and enzymatic inhibitors suggest that RIP1, RIP3, or MLKL could be targeted for treatment of various inflammatory, degenerative, and infectious disorders (Cao & Mu, 2020; Conrad et al. 2016). However, due to the pleiotropic roles of RIP1 and RIP3 in other cellular processes including apoptosis it is difficult to define precisely the participation of necroptosis in multifactorial pathomechanism of neurodegenerative diseases (Degterev et al. 2019; Zhang et al. 2017). Undoubtedly, in recent years necroptosis has become one of the most studied form of cell death, and the inhibition of some elements of this signaling pathway could significantly reduce brain damage (Cao & Mu, 2020). This chapter aims to summarize results of the animal experimental studies which suggest the potential of Nec-1 as a clinically useful neuroprotectant. Data retrieved from PubMed (2005 – March 2021) showed the ability of Nec-1 to ameliorate acute and delayed neuronal cell death induced by hypoxia-ischemia, traumatic brain and spinal cord injury, and some neurodegenerative processes (summarized in Table 1).

2 Characterization of Necrostatin-1

Nec-1 was the first identified necroptosis inhibitor among the tested library of ~15.000 compounds in a phenotypic screen employing human monocytic U937 cell line exposed to TNFα+z-VAD-fmk (Degterev et al. 2005). In parallel, other chemicals (*5-(1H-Indol-3-ylmethyl)-2-thiohydantoins* and *5-(1H-indol-3-ylmethyl) hydantoins*) named necrostatins have been designed and selected in a SAR (structure-activity relationship) study as potent inhibitors of necroptotic cell death induced by TNFα in FADD-deficient Jurkat T cells (Teng et al. 2005). Although various derivatives of Nec-1 as well other inhibitors of necroptosis have been synthesized and investigated in screening necroptotic cellular models, only some of them have been tested in animal studies. Nevertheless, Nec-1 remains the most often used research tool to study the role of necroptosis in various physiological and pathological conditions (Cao & Mu, 2020; Conrad et al. 2016).

2.1 Mechanisms of Necrostatin-1 Action

Nec-1 *(5-(1H-Indol-3-ylmethyl)-(2-thio-3-methyl) hydantoin* or *methyl-thiohydantoin-tryptophan*) is a small-molecule compound (MW = 259.33 g/mol, Fig. 2a). It has been found to be a potent inhibitor of necroptosis without evoking any cytotoxic effects up to 100μM which was superior to some other tested compounds from *5-(1H-indol-3-ylmethyl)-2-thiohydantoin* group (Teng et al. 2005). Later on, Nec-1 and its analogues have been identified as potent allosteric inhibitors of kinase domain of RIP1 (Degterev et al. 2008) and description of the crystal structure of this enzyme facilitated further rational design and development of RIP1 inhibitors (Xie et al. 2013). Nec-1 inhibited TNFα-induced necroptotic cell death with an EC_{50} = 490 nM (Teng et al. 2005, Degterev et al., 2005) and inhibited

Table 1 Neuroprotective effects of Necrotstatin-1 in animal models

Pathology	Model of injury	Animal, weight, n	Dose and route of Nec-1	Effects of Nec-1	Associated mechanisms	References
Brain ischemia	2 h MCAO/R 18 h	Male SV-129 mice; 19–23 g; n = 5–10	i.c.v. 5 min pre- and/or 2–6 h post-; 2–4 ul of 4mM	(−) Infract size ~30% by Nec-1, 7-Cl-Nec-1 and Nec-1s; (+) behavioral improvement; no effect of Nec-1i	(−) LC3II; (+) with z-VAD-fmk	Degterev et al. 2005
	75 min MCAO/R 24 h	Male CD1 mice; 25–30 g; n = 6–7	i.c.v. 6 h post-; 2.6 ug	(−) Infract size ~12%; (+/−) neurological deficits	(+) With humanin; (+) neurological score	Xu et al. 2010
	20 min I/R 12–72 h	Male Sprague-Dawley rats; 280–300 g; n = 3–4	i.c.v. 1 h pre-; 0.1 and 1 ug	(−) Hip. CA1 damage	(−) RIP3; (+) NAD+, (−) cathepsin B	Yin et al. 2015
	15 min I/R 4–60 h	Male Sprague-Dawley rats; 250–300 g; n = 8	i.c.v. 1 h pre-; 1 ug	(−) Hip. damage; (+) memory; (−) anxiety	(−) RIP1/RIP3; (−) pRIP3; (−) RIP3/DAXX	Yang et a. 2017a
	pMCAO/R 4–60 h	Male Sprague-Dawley rats; 250–300 g; n = 10	i.c.v. 10 min pre-; 24 nM	(−) Infract size ~10%; (−) neurological deficits	(−) RIP1; (−) RIP1/RIP3; (−) LC3II; (−) Cathepsin B; (+) MAP-2; (+) GFAP	Ni et al. 2018
	pMCAO/R 24 h	Male CD1 mice; 25–30 g; n = 10	i.c.v. 10 min pre- and 6 h post-; 24 nM	(−) Infract size ~15%	n.s.	Ni et al. 2018
	1 h MCAO/R 24 h-21 days	Male ICR mice; 25–30 g; n = 6	i.c.v. 1 h pre-; 0.04 mg/kg	(−) Neurological deficits; (+) OPCs; (+) myelin	(−) RIP1; (−) RIP3; (−) pMLKL	Chen et al. 2018
	pMCAO/R 24 h	Male ICR mice; 18–22 g; n = 3–10	i.v. 3 post-; 1–10 mg/kg	(−) Infract size ~30% (24 h; 5 and 10 mg/kg); (−) neurological deficits	(−) TNFa; (−) IL-1b; (−) IL-6	Li et al. 2018
	90 min MCAO/R 12 h-28 days	Male Sprague-Dawley rats; 280–320 g; n = 3–10	i.v. 3 post- plus i.p. 1x/day for 7 or 28 days; 10 mg/kg	(−) Infract size ~20% (24 h); (−) neurological deficits	(−) TNFa; (−) IL-1b; (−) IL-6; (−) glia scar	Li et al. 2018
	1 h MCAO/R 6–24 h	Male Wistar rats; 230–280 g; n = 15–20	i.c.v. 1 h pre-; 1 ug	(−) Infract size ~35%; (−) neurological deficits; (+) survival rate	(−) RIP3; (−) MLKL; (+/−) Sirt1	Nikseresht et al. 2019
	30 min MCAO/R 12–72 h	Male Sprague-Dawley rats; 220–250 g; n = 4–7	i.c.v. 30 min pre-; 1.5 ul of 20 mM	(−) Infract size ~40%; (−) neurological deficits; no effect of Nec-1i	(−) pRIP+/NeuN+ cells; (−) pRIP1; (−) RIP3; (−) MLKL; (−) pMLKL; (−) IL-1b	Deng et al. 2019
	1 h MCAO/R 12–48 h	Male ICR mice; 25–30 g; n = 3–7	i.c.v. 5 min. pre-; 3 ul of 4 mM	(−) PI+ cells in striatum; (−) neurological deficits	possible TRAF2/RIP3/MLKL interplay	Li et al. 2019
	90 min MCAO/R 2–48 h	Male Sprague-Dawley rats; 250–300 g; n = 4	i.p. 0.5 µl/g body weight of the 4 mM stock; right and 2 h post-MCAO plus repeated 1× per 12 h	(−) Infract size ~30%; (+) neuronal survival; no effect of Nec-1i	(−) AIF translocation	Mu et al. 2020
	4 h MCAO/R 24 h	Male C57/Bl mice; 20–25 g; n = 5	i.v. after occlusion; RIP1 inhibitor rhTrx1 10 mg/kg	(−) Infract size ~15%; (−) neurological deficits	(−) TNFa; (−) IL-1b; (−) M1/M2 microglia; (−) MMP-9; (−) CCL2	Jiao et al. 2020
Neonatal hypoxia-ischemia	45 min hypoxia	P7 male and female C57B6 mice; n = 7–12	i.c.v. 15 min post NHI; 0.1 µL of 80 uM	(−) Brain damage (P11 and 28), better protection in males → No gender differences	(−) RIP1/RIP3; (−) ROS; (−) NFkB; (−) FLIP; (−) TNFa	Northington et al. 2011
	45 min hypoxia	P7 male and female C57B6 mice; n = 4–14	i.c.v. 15 min post NHI; 0.1 µL of 80 uM	(−) Hippocampal damage; (−) thalamus damage only in males	(−) NO/iNOS; (−) HIF1a/BNIP3; (+) ATP/GSH/MT complex I; (−) GFAP	Chavez-Valdez et al. 2012
	45 min hypoxia	P7 male C57B6 mice; n = 6–8	i.c.v. 15 min post NHI; 0.1 µL of 80 uM	(+) ER morphology; (−) ER stress	(+) BDNF/TrkB in males; (−) p75ntr/Tr.TrkB in females	Chavez-Valdez et al. 2014
	90 or 180 min hypoxia	P7 male and female rats; n = 6	n.s.	n.s.	(−) pPERK2/peIF2α/GADD43; (−) XBP-1	Chavez-Valdez et al. 2016
	LPS + 90 min hypoxia	P12 rats; n = 6	n.s.	n.s. → Brain regions differences	Higher rate of apoptosis and necroptosis in 180 min. hypoxia; sex differences induction of necroptosis and apoptosis; protection by IL-1R antagonist	Askalan et al. 2015 Savard et al. 2015

(continued)

Table 1 (continued)

Intracranial hemorrhages	Intrastriatal IV collagenase Intrastriatal IV collagenase Intrastriatal IV collagenase Endovascular filament Endovascular filament Endovascular filament 200 ul blood into the cisterna magna	Male ICR mice; 25–30 g; n = 6 Male CD1 mice; 8–10 week; n = 10–14 Male ICR mice; 25–30 g; n = 6 Male Sprague-Dawley rats; 300–400 g; n = 6–9 Male Sprague-Dawley rats; 300–320 g; n = 6–14 Male Sprague-Dawley rats; 300–340 g; n = 14–16 Male Wistar rats; 280–350 g; n =	i.c.v. 15 min. pre-; 2.6 ug i.c.v. 2–4 ul of 4 mM i.c.v. 15 min. pre-; 80 nM i.c.v. 30 min post-; 200 ug i.c.v. 30 min post-; 3 ug i.p. 1 h post-; 10.5 mg/kg i.c.v. post-; 3 ug	(−) Injury volume ~30%; (−) PI+ cells (−) Hematoma size; (−) edema; (−) PI+ cells; (−) neurological deficits (−) Hematoma size; (−) edema; (−) PI+ cells; (−) neurological deficits (−) Edema; (−) PI+ cells; (−) neurological deficits (−) Hematoma size; (−) edema; (−) neurological deficits; (−) BBB permeability; (−) PI+ cells (−) Edema; (−) neurological deficits (−) Edema; (−) neurological deficits; (−) TUNEL+ cells	(−) LC3II; (−) Beclin-1; (+) p62; (−) cas-3; (+) Bcl-2 (−) BBB permeability; (−) GFAP (−) Microglia; (−) TNFa mRNA; (−) IL-1b mRNA; (−) RIP1/RIP3/MLKL; (−) NFkB; (−) TNFa; (−) IL-1b (−) RIP3/MLKL; (−) cas-8; (−) MMP-9; (−) TNFa/IL-1b/IL-6; (+) tight junctions (−) RIP1/RIP3; (−) pDrp1/Drp1; (−) NLRP3; (−) cas-1 (−) RIP1/RIP3; (+) synaptic plasticity; (+) pCREB/CREB; (+) BDNF	Chang et al. 2014 King et al. 2014 Su et al. 2015 Chen et al. 2017 Chen et al. 2019 Zhou et al. 2017 Yang et al. 2019a
TBI and SCI	CCI/pneumatic cylinder Closed head injury CCI/ metal impounder Closed head injury Closed head injury Laminectomy/T10 SCI metal rod Laminectomy/Th10 SCI metal rod Laminectomy/Th10 SCI metal rod Laminectomy/Th9 SCI vascular clip Laminectomy/Th8 SCI forceps Laminectomy/Th6-7 SCI vascular clip	Male C57Bl/6 mice; 6–12 weeks; n = 7–9 Male C57Bl/6 mice; 25–30 g; n = 8–13 Male Sprague-Dawley rats; 8 weeks; n = 5–6 Male CD1 mice; 20–25 g; n = 6 Male Sprague-Dawley rats; 280–300 g; n = 4 Male Sprague-Dawley rats; 250–300 g; n = 3–5 Male Sprague-Dawley rats; 250–280 g; n = 6 Male Sprague-Dawley rats; 220–250 g; n = 15 Female ICR mice; 25–30 g; n = 6–8 Male C57Bl/6 mice; 6–8 weeks Female C57Bl/6 mice; 25–30 g; n = 8–9	i.c.v. pre- and post-; 6 ul of 4 mM i.c.v. 5 min. pre-; 4 ul of 4 mM Nec-1s i.c.v. 1 h pre-; 6 ul of 25 mM i.c.v. 15 min pre-; 2.6 ug i.p. co-; 60 ug i.t. 20 min pre-; 1–50 ug i.t. 20 min pre-; 25 ug i.t. 30 min pre-; 50 ug i.t. 5 min post-; 4 ul of 4 mM i.v. 7.8 mg/kg/day; 2× for 5 days i.p. 5 min post-; 5 mg/kg	(−) Lesion volume ~30–40%; (−) PI+ cells; (−) neurological deficits; no effect of Nec-1i (+) Cognitive outcome (−) Lesion volume; (−) neurological deficits; (−) edema (−) PI+ cells (+) Axons; (+) myelin (−) Lesion size; (−) TUNEL+ cells (+) MT morphology (+) Neuronal and astrocyte ER morphology (−) Lesion size; (−) PI+ cells; (+) functional recovery (−) Microglia cell death (−) Edema; (+) motor function	(−) Neutrophils; (−) microglia activation Hip.: (+) pAkt; (+) pmTOR; (+) pS6RP (−) RIP1/RIP3/MLKL; (−) HMGB1; (−) RAGE; (−) NFkB; (−) NLRP3/IL-1b/IL-6 (−) LC3II; (−) Beclin-1; (+) p62; (−) cas-3; (+) Bcl2 (+) MBP; (−) APP; (−) BNIP3 (−) Necroptosis; (−) oxidative stress; (−) neuroinflammation; (−) apoptosis (−) Ca2+; (+) MMP/ATP; (−) cyt.c; (−) Mnf1/Mnf2; (+) Fis1; (+) Tfam/cyt. B Neu: (−) CHOP; (−) Grp78; (−) XBP1 +/− cas-3; +/− TUNEL+cells (−) Grp78; (−) microglia activation; (−) macrophages (−) RIP1; (−) pRIP3; (+) ATP/MMP; (−) ROS/MDA; (+) SOD/GSH	You et al. 2008 Zhu et al. 2014 Bao et al. 2019 Wang et al. 2012 Mu et al. 2021 Wang et al. 2014a Wang et al. 2015 Wang et al. 2017 Liu et al. 2015 Fan et al. 2015 Wang et al. 2019a
Retina injuries	I/R – raised intra-ocular pressure I/R – raised intra-ocular pressure I/R – raised intra-ocular pressure I/R – raised intra-ocular pressure	Male Sprague-Dawley rats; 150–175 g; n = 6–8 Male C57Bl/6J mice; 3 months and P12 Male Sprague-Dawley rats; 250–300 g; n = 5 Male Sprague-Dawley rats; 250–300 g; n = 3	i.v.t. co- or post-; 2 ul of 4 mM i.p. pre- and post-; 2 ug/g/day for 7 days; 7-Cl-Nec-1 i.v.r. post-; 2 ul of 0.1 ug/ml i.p. 5 min post-; 10 and 30 mg/kg RIC	(−) PI+ cells; no effect of Nec-1i (+) Neuronal survival in GCL (+) Neuronal survival in all retina layers (+) Neuronal survival in GCL	(−) LC3II; +/− cas-3; +/− TUNEL+cells (−) Proinflammatory genes (−) RIP1 (−) TUNEL+ in GCL	Rosenbaum et al. 2010 Dvoriantchikova et al. 2014 Kim et al. 2017 Do et al. 2017

	Sodium iodate – AMD model Retinal detachment Retinal detachment Retinal detachment+z-VAD-fmk Tg P23H rhodopsin mutants Blunt ocular injury	Male Sprague-Dawley rats; 330 g; n = 5 Male Brown Norway rats; WT C57BL/6 mice; n = 6–9 Male Sprague-Dawley rats; 260–280 g; n = 6 Male Sprague-Dawley rats; 260–280 g; n = 6 WT and P23H Tg rats; n = 6 P23H knock in mice; n = 5–6 Female Lister Hooded rats; n = 8	i.p. 20–30 mg/kg or 330 μg/ml/day 2 × 3–10 days in eye drops; RIC i.r. co-; 200 uM i.r. co- and 6 h post-; 400 uM i.r. co-; 400 uM s.c. 15 mg/kg/day Nec-1s; from PD21 to PD120 i.v.r. co- and 7 days post-; 5 ul of 3.6 mM; Nec-1s	(+) RPE survival; (+) retinal morphology; (−) degeneration area; (+) visual function no protection alone (+) with z-VAD-fmk → (+) Neuronal survival in ONL; (−) PI+ cells; no effect of Nec-1i (−) PI+ cells; (−) cytotoxicity of z-VAD-fmk (+) ONL thickness; (−) TUNEL+ cells; (+) vision (+) RGCs loss in center; +/− vison; +/− ONL thickness	(−) RIP1 activity; effective also in rabbits and mini-pigs (−) TUNEL+ cells; (+) ONL thickness; (−) CD11b+ cells; (−) ROS; (−) AIF (−) pRIP1 (−) pRIP1; (−) LC3II (−) RIP1/RIP3; (−) ROS; (−) NLRP3/IL1-b; (−) Iba1+ cells; (−) pNFkB; (−) IL-1a n.s.	Jang et al. 2019 Trichonas et al. 2010 Dong et al. 2012 Dong et al. 2014 Viringipurampeeret al. 2016 Thomas et al. 2019
Alzheimer's disease	Tg (APPswe, PS1dE9) Ab-infusion i.c.v. Tg (APPswe, PS1dE9) i.c.v. AlCl3 (2 ul of 2 mM) i.c.v. AlCl3 (0.5% for 5 days) LPS (15 ug i.c.v.) High fat diet (21 weeks) D-galactose/2 months plus hepatectomy	Tg APP/PS1 and WT C55Bl/6 mice; n = 6–7 Male ICR mice; n = 6–7 Tg APP/PS1 and WT C57Bl/6 mice; n = 10 Male ICR mice; 30–35 g Male KM mice; 25–30 g; n = 10 Male Wistar rats; 250–280 g; n = 8 Male rats; n = 8 Male C57Bl/6 mice; 20–25 g; n = 7–12	i.v. 6.25 mg/kg, twice a week from 4 to 7 months i.v. 7 days pre- and 7 days post-; 6.25 mg/kg/twice a week i.v. 6.25 mg/kg, twice a week from 7 to 8 months i.c.v. co- or post-; 2 ul of 4 and 8 mM i.c.v. co-; 3 ul of 4 mM/day for 5 days i.c.v. co-; 10 uM s.c. 1.65 mg/kg/day, from 13 to 21 week i.p. 5 min pre-; 6.25 mg/kg	(+) Spatial memory (−) Memory deficits (−) Plaques (−) Memory deficits; (+) neuronal survival in CA3; no effect of post-treatment (2–8 h) (+) Neuronal survival; (−) memory deficits (−) Memory deficits (+) Cognitive function; (+) synaptic plasticity; (−) microglia activation (−) Neuronal loss; (−) PI+ cells; (−) microglia activation	(−) Ab plaques; (−) Ab oligomers; (−) Tau; (−) pRIP1; (−) cas-3; (+) Bcl2 n.s. (−) pRIP3; (−) Bax; (+) Bcl2 (−) RIP1; (−) cas-3; (−) LC3II; (−) Tau; (−) Ab; +/− NFkB (−) RIP1; (−) cas-3; (−) LC3II; +/− NFkB; (+) with z-VAD-fmk (−) RIP1/RIP3; (−) cas-8/cas-3; (−) MDA; (+) SOD/GSH/catalase; (−) GLUD/GLUL (−) RIP1/RIP3; (−) ROS; (−) MT swelling; (−) Tau; (−) NFkB; +/− apoptosis (−) RIP1; (+) GluA1; (−) TNFa/IL-1b; +/− NFkB	Yang et al. 2017b Yang et al. 2017b Yang et al. 2019b Qinli et al. 2013 Hao et al. 2020 Nikseresht et al. 2015 Jinawong et al. 2020 Duan et al. 2018
Parkinson's disease	MPTP (i.p. 20 mg/kg, 5 days) MPTP (i.p. 40 mg/kg) MPTP (i.p. 20 mg/kg, every 2 h up 8 h) 6-OHDA (4 ug, into right striatum) MPTP (i.p 30 mg/kg for 5 days)	C57Bl/6 mice; 9 week old; n = 8 C57Bl/6 mice; 13 week old; n = 6–7 C57Bl/6 mice; 8–10 week old; n = 6 C57Bl/6 mice; 12 week old; n = 3–10 C57Bl/6 mice; 6 month old; n = 5–8	i.c.v. 1 ug/day Nec-1; i.p. 10 mg/kg/day Nec-1s; from 3 to 21 days i.p. 1 h post-; 10 mg/kg/day Nec-1s up to 30 days i.p. 1.65 mg/kg/day; 1 h pre- and post- up to 21 days i.p. 8 mg/kg/day Nec-1s, 3 days before surgery and 7 days after n.s.	(+) TH+ in SNpc; (+) striatal DA fibers +/− TH+ in SNpc (+) TH+ in SNpc; (+) DA level in Str (+) TH+ in SNpc; (+) striatal DA fibers; (+) motor performance Protection by AgomiR-425	(−) ROS less damage in RIP3-/- mice less damage in RIP3-/- or MLKL -/- mice; (−) TNFa/IL-1b/IL-6 (+) axons miR-425 negative regulator of RIP1	Iannielli et al. 2018 Dioniso et al. 2019 Lin et al. 2020 Onate et al. 2020 Hu et al. 2019
ALS and other neuropathies	OPTN-/- and Tg SOD1(G93A) OPTN-/- and Tg SOD1(G93A) Tg SOD1(G93A) sciatic nerve chronic constriction (CCI)	WT and mutant mice; n = 5 WT and mutant mice; n = 6–23 WT and mutant mice; n = 12	Oral dosing, 2.5–5 mg/day Nec-1s; for 1 month from 8 weeks of age n.s. n.s. i.p. 0.2-0.4 mg/kg/day for 21	(+) Motor neurons; (−) demyelination; (+) motor performance No protection by RIP3 removal in SOD1(G93A) or OPTN-/- mice No protection by MLKL removal in SOD1(G93A) (−) Mechanical and thermal allodynia; (−) PI+	(−) TUNEL+ cells; (−) axonal loss n.s. n.s. (−) RIP1/RIP3; (−) NFkB; (−) TNFa/IL-1b; (−) substance P	Ito et al. 2016 Dermentzaki et al. 2019 Wang et al. 2020 Liang et al. 2019

(continued)

Table 1 (continued)

	ouabain (auditory neuropathy model) ouabain (auditory neuropathy model) mechanical sciatic and optic nerve injury (*ex vivo*)	Male Sprague-Dawley rats; 230–240 g; n = 6 Male Sprague-Dawley rats; 250–300 g; n = 4–8 Male Sprague-Dawley rats; 250–300 g; n = 4 Nerve explants from C57Bl/6 mice; 25 g; n = 3	days Local, 10 min post-; 10 ul of 2 mM Local, 10 min post-; 10 ul of 2 mM co-; 100 uM	cells (+) SGC density; (−) hearing loss In RIP3 overexpressed animals: (+) SGC density; (−) hearing loss (−) Axonal degeneration; (+) electrophysiological activity	(−) RIP3; (+) with z-VAD-fmk Less hearing loss and SGCs damage in RIP3-/- (−) Mitochondrial fragmentation in axons	Wang et al. 2014b Wang et al. 2021 Arrazolla et al. 2019
Other neurodegenerative diseases	Tg R6/2 mice Npc1-mutant mice EAE model	WT and mutant mice; n = 6–7 WT and mutant mice; n = 10 Female C57Bl/6 mice; 18–20 g; n = 8	i.c.v. in osmotic pumps from 5 to 11 week i.p. 90 and 180 mg/kg/day; every 2nd day from 3 to 7 week old i.t. 1.65 mg/kg from day 2 every 3 days for 15 days	(+) Animal weight; (+) motor function; (−) disease onset (+) Lifespan; (−) neurological symptoms; no effect of Nec-1i (−) Clinical score; (−) lesions; (−) cell infiltrates	n.s. (−) Purkinje cell loss (−) pMLKL/MLKL; (−) pDrp1/Drp; (−) Bax/Bcl2; (−) Bim; (−) TNFa/IL-1b/INFg	Zhu et al. 2011 Cougnoux et al. 2016 Wang et al. 2019b

(−) reduction/inhibition, (+) increase/stimulation, +/− no effect, *GCL* ganglion cell layer, *hip.* hippocampal, *I/R* ischemia/reperfusion, *i.c.v.* intracerebroventrical, *i.p.* intraperitoneally, *i.r.* intraretinal, *i.t.* intrathecal, *i.v.* intravenous, *i.v.r.* intravitreal, *MCAO* middle cerebral artery occlusion, *ONL* outer nuclear layer, *OPCs* oligodendrocyte precursor cells, *P* postnatal day, *PI* propidium iodide, *pMCAO* permanent MCAO, *s.c.* subcutaneous, *SCI* spinal cord injury, *SGC* spiral ganglion cells, *TBI* traumatic brain injury, *WT* wild type

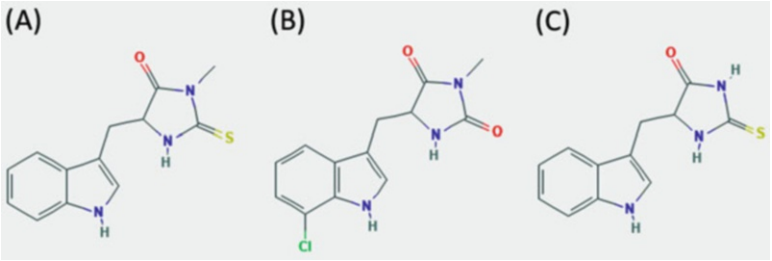

Fig. 2 Chemical structure of chosen members of Necrostatins family: (**a**) Necrostatin-1 (Nec-1); (**b**) Necrostatin-1 stable (Nec-1s, 7-Cl-O-Nec-1, Nec-2); (**c**) Necrostatin-1 inactive (Nec-1i). (Source: https://pubchem.ncbi.nlm.nih.gov)

RIP1 kinase activity in in vitro assay with $EC_{50} = 182$ nM (Degterev et al. 2008), suggesting a good correlation between these two processes. Because of its ability to stop RIP1 autophosphorylation and consequently to prevent its interaction with RIP3 and subsequent formation of necrosome and MLKL activation, Nec-1 for many years has been regarded as a potent inhibitor of RIP1-RIP3-MLKL signaling (Degterev et al., 2008, Takahashi et al. 2012). However, being a RIP1 inhibitor, Nec-1 apart from necroptosis could also inhibit RIP1-dependent apoptosis (Cao & Mu, 2020; Conrad et al. 2016).

In order to verify Nec-1 specificity as a necroptosis inhibitor, its two analogs, namely Nec-1 stable (Nec-1 s, 7-Cl-O-Nec-1, Nec-2) (Fig. 2b) and Nec-1 inactive (Nec-1i) (Fig. 2c), were investigated in parallel with the parent drug (Degterev et al., 2005). They were chosen in a wide structure-activity relationship (SAR) study which revealed that elimination of methyl group in the hydantoin moiety of Nec-1 reduced its antinecroptotic activity (Nec-1i). Interestingly, an addition of chlorine group to the phenyl ring and substitution of sulfur to oxygen in the hydantoin moiety (Nec-1 s) improved ten times Nec-1 inhibitory effect on RIP1 activity ($EC_{50} = 18$ nM) (Degterev et al. 2008) and 2–10 times increased its protective potency in cellular models of necroptosis (Degterev et al. 2005, Teng et al. 2005). However, such differences in the potency of action of Nec-1 derivatives not always have been observed in vivo at least after their direct administration to the brain. For example, in the mouse brain ischemia model (MCAO, middle cerebral artery occlusion) an intracerebroventrical (*i.c.v.*) administration of Nec-1, 7-Cl-O-Nec-1 and Nec-1 s (2–4μl of 4 mM) to a similar extent reduced infarct volume and improved neurological score (Degterev et al., 2005).

Besides inhibiting RIP1 kinase, Nec-1 is also a potent inhibitor of indoleamine 2,3-dioxygenase (IDO) ($EC_{50} = 116\mu M$) which may contribute to its mechanism of action in inflammatory and neurodegenerative processes (Zhang et al. 2017, Zhao et al. 2015). Takahashi et al. (2012) compared Nec-1, Nec-1 s, and Nec-1i with respect to their effect on IDO activity and on necroptotic cell death inhibition, and found that Nec-1 was identical in terms of the chemical structure to *methyl-thiohydantoin-tryptophan* (MTH-Trp), an inhibitor of IDO. They found that both Nec-1 and Nec-1i inhibited human IDO activity with similar potency ($EC_{50} \sim 116\mu M$)

as did 1-methyl-tryptophan (1-MT, EC_{50} ~ 143μM), an IDO inhibitor, whereas Nec-1 s was devoid of such activity (Takahashi et al. 2012). Although the IDO inhibitor 3-MT was not protective in the mouse cellular necroptosis assay (L929 cells exposed to recombinant human TNFα), Nec-1i was only 10× less potent than Nec-1 or Nec-1 s and was equipotent at high concentrations in the inhibition of necroptotic cell death (Takahashi et al. 2012). It is in contrast to findings from human cell–based models of necroptosis where Nec-1i was ineffective (Degterev et al., 2005, Teng et al. 2005). Moreover, in vivo high doses (6 mg/kg) of Nec-1, Nec-1i, and Nec-1 s given intravenously (*i.v.*) prevented the mortality associated with TNFα-induced systemic inflammatory response syndrome (SIRS) equally well, but, paradoxically, low doses of Nec-1 or Nec-1i (0.6 mg/kg) sensitized mice to TNFα-induced mortality. The abovementioned data question the relevance of using Nec-1i as a negative control for necroptosis in in vitro and in vivo studies (Takahashi et al. 2012) suggesting that species differences and/or route of administration could influence Nec-1i effects. Since Nec-1 s did not exhibit low-dose toxicity in SIRS model, it has been suggested to be preferentially used in animal studies (Takahashi et al. 2012). Since inflammation significantly contributes to the development and progression of age-related neurodegenerative diseases (Fan et al. 2017, Zhang et al. 2017), the additional activity of Nec-1 on IDO could be rather favorable when considering Nec-1 as an efficient neuroprotectant.

2.2 Pharmacokinetics of Necrostatin-1

Pharmacokinetics and bioavailability of Nec-1 in Sprague-Dawley rat plasma has been evaluated by Geng et al. (2017) using LC-MS/MS method. It seems that Nec-1 remains stable in plasma in different processing and storage environmental conditions. The plasma concentration of Nec-1 was determined in rats who received a single dose via intravenous and oral route (5 mg/kg), respectively. A two-compartment model fitted the concentration-time profile of the Nec-1 with C_{max} 1733 μgL-1 and t1/2 1.8 h for intravenous route, and C_{max} 648 μgL-1 and t1/2 1.2 h for oral route, respectively. The results showed that absolute bioavailability of Nec-1 was 54.8% (Geng et al. 2017). In an analytical study using the original HPLC-Q-TOF method, Mikuš et al. (2018) measured Nec-1 s plasma concentrations in Wistar rats 50 min after *i.v.* bolus dose (0.37 mg/kg) administration which was ca. 105 ng/ml (377 nM). However, it is difficult to compare pharmacokinectic properties of Nec-1 and Nec-1 s since there are no studies where both compounds would be tested under the same experimental conditions. Data on BBB (blood-brain barrier) crossing by Nec-1 are rather limited. In the early study on necroptosis, Teng et al. (2005) reported that Nec-1 after *i.v.* administration (dose 1 mg/kg) in CD1 mice had rather moderate pharmacokinetic characteristics (C_{max} 873 ngL-1 and t1/2 67 min) with significantly higher removal rate in females, but it readily entered the CNS (after 30 min 0.74μM brain concentration) showing a good brain-to-plasma ratio (2.4). However, the compound was metabolically unstable and was relatively quickly cleared from the body (within 180 min) (Teng et al. 2005).

Apart from low metabolic stability, another important drawback of Nec-1 as potential clinical therapeutic is related to its low solubility in water. Usually for in vitro studies, stock solutions of this compound are prepared in DMSO (>10 mg/kg) (Degterev et al. 2008, Jantas et al. 2020) whereas for in vivo studies DMSO, ethanol, or PEG400 are used (Dionísio et al., 2019, Geng et al. 2017, Mikuš et al. 2018, Nikseresht et al. 2015). This poor physicochemical property of Nec-1 requires the usage of relevant vehicles for control groups (percentage of the solvent can reach 1–3% in vitro and up to 20% in vivo), which by itself could affect the outcome in particular experimental models of human pathologies (Geng et al. 2017, Mikuš et al. 2018).

3 Neuroprotection by Necrostatin-1 in Animal Models

3.1 Brain Ischemia

During brain ischemia (stroke) occurs the breakdown of neuronal cellular integrity by ionic imbalance, energetic collapse, excitotoxicity, and increased ROS production. These factors lead to neuronal cell damage executed via rapid nonspecific necrosis (cell lysis) in ischemia core and by programmed cell death pathways (apoptosis or necroptosis) in the penumbra region. Moreover, the injury-induced neuroinflammatory processes could worsen the extent of brain damage and neurological deficits evoked by this life-threatening episode (Mehta et al. 2007). The first evidence that necroptosis contributes to delayed ischemic brain injury in vivo in mice through a mechanism distinct from apoptosis and that it offers a new therapeutic target for stroke with an extended window for neuroprotection was provided by Degterev et al. (2005). In mice exposed to transient focal cerebral ischemia (MCAO) Nec-1, 7-Cl-Nec-1 and Nec-1 s but not Nec-1i (*i.c.v.* 2–4 ul of 4 mM) given before and after (during infusion and reperfusion) occlusion to similar extent (~30%) reduced infract volume and improved neurological deficits (Degterev et al. 2005). Further tested compound, 7-Cl-Nec-1 was also effective when given 2 and 6 h after MCAO and its administration was associated with the inhibition of autophagy induced during reperfusion time. Interestingly, the pan-caspase inhibitor z-VAD-fmk was protective when given 2 but not 6 h after occlusion but it synergized with Nec-1 in protection at both time points (Degterev et al. 2005). These data encouraged further animal research aiming to prove neuroprotective potency of Nec-1 and its derivatives for stroke management. In line with the studies postulating that the combination therapy rather than monotherapy may be required for efficient neuroprotection in brain ischemia, Xu et al. (2010) evaluated protective effects of combined treatment with Gly(14)-humanin (*i.c.v.* 0.1μg) and Nec-1 (*i.c.v.* 2.6μg) in the mouse transient MCAO model (75 min occlusion and 24 h reperfusion). They showed that administration of humanin or Nec-1 alone 4 h after MCAO moderately reduced cerebral infarct volume (~12%) but combined treatment with both agents to a higher extent decreased lesion size (up to 20%) and most importantly improved also neurological score (Xu et al. 2010).

Using the rat model of global cerebral ischemia (four-vessel occlusion) followed by reperfusion (I/R model), Yin et al. (2015) found that Nec-1 (*i.c.v.* 0.1 and 1μg) administered 1 h before ischemia in a dose-dependent manner protected hippocampal CA1 neurons which was accompanied by a decrease in expression and nuclear translocation of RIP3, increased NAD+ level, and attenuated cathepsin B (Yin et al. 2015). In a similar experimental model, Yang et al. (2017a) showed that 1 h pretreatment with Nec-1(*i.c.v.* 1μg.) 5 days after induction o I/R prevented locomotor deficit, relieved anxiety behavior, and improved cognitive functions in rats. Moreover, Nec-1 protected neurons in the hippocampal CA1 region against ischemic damage through newly identified RIP3 nuclear substrate DAXX (death associated protein) which appeared to play an important role in I/R-induced neuronal death (Yang et al. 2017a). In another study, Ni et al. (2018) in the permanent MCAO model in rats found that Nec-1 (*i.c.v.* 24 nM) pretreatment (10 min before MCAO) or RIP1 knockdown (shRNA RIP1 given 5 days before MCAO) were protective and attenuated neurological deficits. This beneficial effect of Nec-1 was evidenced in the ischemic cortex by the reduced infarct volume (~10%), improved neuronal (MAP-2) and astrocyte (GFAP) survival, decreased RIP1–RIP3 interaction, and attenuated level of autophagy (LC3II) and lysosomal (cathepsin B, lysosomal membrane permeability) markers. Moreover, they confirmed protective effects of Nec-1 in the mouse pMCAO model where this compound was effective (~15% reduction of infarct volume) in pretreatment (10 min before MCAO) and posttreatment (6 h after MCAO) schedules (Ni et al. 2018).

Ischemic stroke, apart from neuronal and astrocyte damage, can also cause a severe injury to white matter, especially to oligodendrocyte precursor cells (OPCs) and premature oligodendroglia. Chen et al. (2018) showed that Nec-1 (*i.c.v.* 0.04 mg/kg) injected to mice 1 h before the onset of 60-min MCAO followed by 24 h reperfusion, 21 days after injury significantly promoted OPC survival, alleviated white matter injury, and improved cognitive function. It was accompanied by a decrease in RIP1, RIP3, and pMLKL expression in the subventricular zone and corpus callosum (Chen et al. 2018). In another study, a novel analogue of Nec-1, DTIO was tested in the mouse and rat brain ischemia models (Li et al. 2018). In the mouse permanent MCAO model, DTIO (*i.v.* 5 and 10 mg/kg, given 3 h after the occlusion) reduced brain damage by about 30% and attenuated neurological deficits. The same group tested the DTIO (10 mg/kg) effect in the rat transient MCAO model (90 min MCAO) where this compound was given *i.v.* 3 h after MCAO and starting from day 2 it was administrated intraperitoneally (*i.p.*) once a day for 28 days. At these two end points DTIO significantly reduced infarct volume (~20% at 24 h) and improved neurological performance without influencing cerebral blood flow. Moreover, DTIO inhibited ischemia-induced release of pro-inflammatory cytokines (TNFα, IL-1β, and IL-6) in the cerebral cortex 12 h and 7 days after the induction of permanent or transient ischemic episodes, respectively. Moreover, in a rat model DTIO prevented the formation of glial scar as found 7 days after MCAO by evaluation of expression of astrocytic markers (GFAP, phosphacan and neurocan) (Li et al. 2018).

A relationship between sirtuin 1 (Sirt1), a member of histone deacetylase class III, and the necroptosis signaling pathway and its downstream events has been explored

by administration of ex-527 (selective and potent inhibitor of Sirt1) and Nec-1 in the rat model of focal cerebral ischemia (Nikseresht et al. 2019). They demonstrated that 60 min pretreatment with Nec-1 (*i.c.v.* 1 μg) reduced the infarct volume of ischemic brains to a significantly higher extent (~35%) than the inhibitor of Sirt1 (10μg, ex-527) did. Although both agents reduced RIP3 and MLKL in the prefrontal cortex and hippocampus, Nec-1 did not affect Sirt1 expression. Moreover, both agents improved survival rate, but only Nec-1 attenuated stroke-associated neurological deficits (Nikseresht et al. 2019). A direct in vivo evidence that phosphorylated RIP1 (Ser 166) plays an important role in the initiation of RIP3/MLKL-dependent necroptosis in the pathogenesis of ischemic stroke in the rodent brain was provided by Deng et al. (2019). In the rat MCAO model they found that Nec-1 but not Nec-1i (*i.c.v.* 1.5μl of 20 mM) given 30 min before occlusion reduced infract volume by about 40% and attenuated ischemia-associated neurological deficits. It was accompanied with a decrease in the number of p-RIP1-positive neurons and amelioration of p-RIP1, RIP3, MLKL, p-MLKL, and mature IL-1β expression, suggesting a direct interplay between RIP1 and inflammation after I/R (Deng et al. 2019).

Some brain ischemia studies brought new findings about new regulators of necroptosis. For example, Li et al. (2019) showed an interplay between TRAF2 and RIP3 and MLKL in the mouse transient MCAO model. The TRAF2 expression was induced by MCAO at 24 h after reperfusion in cortical and striatal neurons and microglia. Interestingly, only striatal knockdown of TRAF2 increased the infarct size and cell death which was associated with microglial activation and increased expression of pro-inflammatory cytokines (TNFα, IL-1β and CD32). In this model, Nec-1 (*i.c.v.* 3μl of 4 mM) given just before occlusion reduced the neurological deficits induced by ischemia and decreased the number of necrotic (PI-positive) cells in the striatal regions in wild type and TRAF2−/− mice (Li et al. 2019). Mu et al. (2021) in the rat transient MCAO model showed that *i.p.* injection of Nec-1 but not Nec-1i (0.5μl/g body weight of the 4 mM stock solution right after occlusion, repeated at 2 h after the onset of reperfusion and once every next 12 h) significantly reduced the infarct area (by about 30%) and increased the survival of neurons. Moreover, this effect was accompanied by the inhibition of AIF nuclear translocation induced by I/R (Mu et al. 2021). Nec-1 may also provide neuroprotection in ischemic stroke through reduction of microglial neuroinflammation. To this end, Jiao et al. (2020) showed in the transient MCAO model in mice that recombinant human thioredoxin-1 (rhTrx-1, a putative RIP1 inhibitor, *i.v.* 10 mg/kg, given just after occlusion) significantly reduced the infarct volume (~15%) and improved neurological functions. It was associated with changes in microglia polarization (decrease in M1 and increase in M2 phenotypes) and attenuation of inflammatory cytokines (TNFα and IL-1β) (Jiao et al. 2020).

3.2 Neonatal Hypoxia-Ischemia

Neonatal hypoxia-ischemia (NHI) is a trigger of necrosis and a continuum of hybrid cell death programs where excitotoxicity, oxidative injury, and inflammation are

thought to play the prominent role in histopathological and behavioral consequences of this acute brain damage. NHI is often modeled in rodents by unilateral carotid artery ligation followed by 45–180 min hypoxia which can produce moderate-to-severe injury in cortical, striatal, and hippocampal brain regions in immature rodents (usually mice or rats at postnatal day 7, P7). The first study evidencing the neuroprotective efficacy of Nec-1 in NHI was carried out by Northington et al. (2011). They showed that a single *i.c.v.* injection of Nec-1 (0.1μL of 80μmol) in P7 C57B6 mice directly after NHI (45 min hypoxia) significantly decreased injury in the forebrain and thalamus at P11 (4 days after NHI) and P28 (3 weeks after NHI) and this effect was more pronounced in males. Further biochemical study performed 3 and 24 h after NHI revealed that Nec-1 inhibited RIP1-RIP3 complex formation, attenuated oxidative stress markers, and attenuated NFκB activity and inflammatory response (TNFα, IL-1β, IL-6, IL-12) (Northington et al. 2011). In the next study, the same group further explored biochemical processes associated with neuroprotective action of Nec-1 by investigation of mitochondrial dysfunction in neurons and astrocytes after NHI in P7 male and female mice (Chavez-Valdez et al. 2012). Nec-1 immediately after NHI (3–24 h) regardless of gender attenuated oxidative stress and mitochondrial injury as evidenced by prevention of nitric oxide (NO•) production, iNOS (inducible nitric oxide synthase) activation, attenuation of glutathione oxidation, upregulation of HIF-1α (hypoxia inducible factor-1 alpha) and BNIP3 expression, decline in mitochondrial complex-I activity, decrease in ATP levels, and mitochondrial structural pathology in astrocytes and in neurons. Moreover, Nec-1 at P11 decreased astrogliosis (GFAP level) induced by NHI (Chavez-Valdez et al. 2012). The next report from the same team showed that in both sexes NHI acutely (24 h) increased BDNF levels in the forebrain but not in the diencephalon which was followed by the delayed decrease (96 h) and late recovery (21 day). Nec-1 prevented the decrease in BDNF levels in the forebrain while increased its levels in the diencephalon. At the level of *Bdnf* gene, Nec-1 induced its expression after 96 h in the diencephalon in both sexes whereas in the forebrain region only in male mice. Moreover, only in female mice, NHI increased p75ntr and truncated TrkB levels which were attenuated by Nec-1 but in male mice Nec-1 preserved BDNF levels and TrkB activation. Finally, Nec-1 attenuated hippocampal cell damage after NHI in male and female mice, however, in the thalamus only in the former ones. Thus, it has been concluded that the regional differences in BDNF levels may be a consequence of injury severity after NHI, but sexual differences in response to Nec-1 may represent a differential thalamo-cortical preservation or alternatively off-target regional effect of Nec-1 (Chavez-Valdez et al. 2014). Importantly, Nec-1 helped verify the hypothesis that the ER stress is a prominent feature of delayed neuronal death via programmed necrosis after neonatal NHI. Nec-1 attenuated biochemical markers of ER stress (PERK and eIF2α phosphorylation, GADD43 and unconventional XBP-1 splicing) after NHI as well as rescued ER morphological changes induced by NHI at delayed stages (Chavez-Valdez et al. 2016).

A still unsolved problem is to what extent necroptosis and apoptosis can overlap and which elements of these two death signaling pathways are critical for their

interaction in hypoxic cells. Askalan et al. (2015) studied the role of apoptotic and necroptotic processes in two models of NHI in P7 rats inducing mild-moderate (90 min) or severe (180 min) hypoxia. It was observed that 7 days after injury in severe hypoxia model there were more lesions with higher rate of apoptotic (caspase-3 and AIF dependent) and necroptotic (RIP3) cell death. Moreover, in males, but not in females, apoptosis was more profound in rats exposed to the mild-moderate hypoxia as compared to results obtained in the severe NHI model. These findings justify further the evaluation of Nec-1 or other necroptosis inhibitors in NHI by employing models of various severities and highlight the need for continuation of research on both sexes. Another interesting point is that hypoxia-ischemia combined with inflammation is an important cause of neonatal encephalopathy which affects up to 1% of newborns and over a longer period of time leads to cerebral palsy. It can be modeled in animals by treatment with LPS and exposure to hypoxia-ischemia. In the study by Savard et al. (2015), the induction of necroptotic (increased RIP3) and apoptotic (caspase-3 activation) processes was observed in P12 rat pups treated for 4 h with LPS (200μg/kg *i.p.*) followed by 1.5 h hypoxia-ischemia. In that model, the authors uncovered a new paradigm of neuronal self-injury orchestrated by neuronal synthesis of IL-1β and MMP-9 and observed the protective effect of systemically administered IL-1 receptor antagonist (IL-1Ra) (Savard et al. 2015). It is expected that Nec-1 should be beneficial also in such model, since reports from brain ischemia models showed modulating effects of Nec-1 on inflammatory response and MMP-9 activity.

3.3 Intracranial Hemorrhages

Intracranial hemorrhages comprise intracerebral hemorrhage (ICH), intraventricular hemorrhage, and subarachnoid hemorrhage (SAH) and are life-threatening neurological diseases characterized by high mortality and morbidity. They can occur as a result of head injury or spontaneously, usually from a ruptured cerebral aneurysm. Unfortunately, to date, limited therapeutic options are available for management of intracranial hemorrhages (Fang et al. 2020). Since many studies showed involvement of nonapoptotic forms of programmed cell death including necroptosis and neuroinflammation in the pathophysiology of intracranial hemorrhages, some research has been done on Nec-1 effects in ICH and SAH animal models. The first study addressing this issue was conducted by Chang et al. (2014) who used the mouse ICH model induced by unilateral intrastriatal infusion of type IV collagenase. They showed that *i.c.v.* injection of Nec-1 (2.6μg) 15 min before ICH reduced the injury volume and number of PI-positive cells and prevented changes induced by ICH in autophagy (LC3-II, Beclin-1, p62)- and apoptosis (Bcl-2 protein level and decreased cleaved caspase-3)-associated proteins at 24 and 72 h after ICH. These data showed that a cross talk existed among necroptosis, apoptosis, and autophagy after ICH and Nec-1 to some extent could suppress the activation of these cell death pathways (Chang et al. 2014). In another study employing the same ICH model King et al. (2014) demonstrated that Nec-1 and Nec-1i (*i.c.v.* 2–4μl of 4 mM)

administrated at the time of injury completely reduced hematoma size at 72 h. However, only Nec-1 improved neurological outcome in this model which was associated with the reduced number of PI-positive cells, preserved BBB permeability, and decreased astrogliosis and brain edema (King et al. 2014). Moreover, Su et al. (2015) demonstrated that Nec-1 pretreatment improved neurological function and attenuated brain edema in mice after ICH via reduction of RIP1-RIP3 interaction and PI-positive cells, and inhibited microglia activation and expression of pro-inflammatory genes (TNFα and IL-1β).

Regarding in vivo models of SAH, Chen et al. (2017) demonstrated an increase in expression of necroptosis proteins (RIP1, RIP3, and MLKL) during brain injury (after 3–48 h) evoked by endovascular perforation (endovascular filament model) in rats. Further, they found that Nec-1 (*i.c.v.* 200μg; given 30 min after injury) partially attenuated brain swelling, reduced the lesion volume, reduced the number of PI-positive cells, and improved neurologic outcomes. These effects were accompanied by reduced expression of necroptosis proteins, inhibited NFκB nuclear translocation, and reduced release of pro-inflammatory cytokines (TNFα and IL-1β). In the next study, these findings were confirmed using a wider range of methods and measured parameters. The beneficial effect of 1 h pretreatment with Nec-1 was confirmed by reduction in lesion size and ventricle volumes (MRI method), which ameliorated albumin leakage and the degradation of tight junction proteins (ZO-1, occludin and claudin-5). Nec-1 inhibited the production of the pro-inflammatory cytokines (IL-1β, IL-6, and TNF-α) and reduced expression and activity of MMP-9 (Chen et al. 2019). In another study, Zhou et al. (2017) using the SAH rat model studied interactions between the RIP1-RIP3-DRP1 pathway and NLRP3 inflammasome. Nec-1 or mitochondrial division inhibitor (Mdivi-1) administered *i.p.* 1 h after SAH alleviated brain edema and neurological deficits measured after 24 h. It was accompanied by reduced RIP1, RIP3, phosphorylated DRP1, and NLRP3 inflammasome (Zhou et al. 2017). Further in vivo study in rats where SAH was induced by a double injection of autologous blood (200 μl) into the cisterna magna, Nec-1 (*i.c.v.* 3μg) alleviated brain edema and improved neurobehavioral scores. Apart from decreasing the hippocampal expression of RIP1 and RIP3, Nec-1 improved synaptic connectivity (PSD-95, Neurexin-1 and Neuroligin-1) and activated CREB-BDNF pathway (Yang et al. 2019a). Collectively, the data clearly indicate that Nec-1 could be protective in experimental animal models of intracranial hemorrhages engaging various mechanisms and underline the necessity of development of new RIP1 inhibitors with better pharmacokinetic properties for clinical purposes.

3.4 Traumatic Brain and Spinal Cord Injuries

A growing body of evidence indicates that necroptosis together with apoptotic and autophagic cell death play an essential role in the mechanism of neuronal death after traumatic brain (TBI) and spinal cord injury (SCI). Direct mechanical trauma to the brain or to the spinal cord causes the primary injury and sets off a complex of toxic

mediators, cytokines, and free radicals which induce the secondary injury executed by apoptotic and nonapoptotic forms of cell death. The first report demonstrating that Nec-1 could be protective in TBI was published by You et al. (2008). They showed in the controlled cortical impact (CCI) model in mice that pre-(5 min) and post-(5–15 min but not 30 min) treatment with Nec-1 (*i.c.v.* 4μl of 4 mM) but not with Nec-1i reduced histopathological and functional deficits in mice lasting up to 35 days after injury. It was associated with reduced lesion (by about 30–40% in the pretreatment schedule), decreased number of PI-positive cells in the cortex and hippocampus, and attenuated neuroinflammation and astrogliosis without influence on caspase-3 level. These results suggested that Nec-1 might be a novel therapeutic agent with pleiotropic action which could be considered for the treatment of head injury and other acute CNS disorders (You et al. 2008). Using the same TBI model, Zhu et al. (2014) demonstrated an increase in Akt and mTOR signaling in cortical and hippocampal regions 24 h after CCI. Pretreatment with Nec-1 s (*i.c.v.* 4μl of 4 mM) further increased hippocampal Akt and improved place learning, and these beneficial effects were reduced by rapamycin or Akt inhibitor (Zhu et al. 2014). Finally, Bao et al. (2019) showed in CCI TBI model that Nec-1 (*i.c.v.* 6μl of 25 mM solution) and melatonin but not the caspase inhibitor z-VAD-fmk reduced cortical lesion volume, attenuated brain edema, and improved motor ability and learning and memory. It was accompanied with alleviated necroptotic markers (RIP1, RIP3, and MLKL) in the hippocampus and cortex and reduced the number of TUNEL-positive cells without affecting caspase-3-positive ones. Moreover, Nec-1 and melatonin reduced HMGB1 and RAGE levels, NFκB activation, and neuroinflammatory proteins (IL-1β, IL-6, and NLRP3) in both studied brain regions. They also found that TNFα-induced protein 3 (TNFAIP3) was indispensable for regulating and controlling necroptosis and inflammation after CCI, and that the lack of TNFAIP3 A20 led to aggressive necroptosis and attenuated the anti-necroptotic effects of Nec-1 and melatonin (Bao et al. 2019). In another type of TBI model, namely the closed head TBI model (a weight-drop model), Wang et al. (2012) aimed to explore the effect of Nec-1 on apoptosis and autophagy. They demonstrated in mice that 15 min pretreatment with Nec-1 (*i.c.v.* 2.6μg) attenuated TBI-induced cortical and hippocampal injury after 24 h and it was associated with reduced levels of autophagic (LC3II, p62, and Beclin-1) and apoptotic (caspase-3 and Bcl-2) markers (Wang et al. 2012). In another study employing the same type of TBI but this time in rats, Mu et al. (2021) demonstrated a beneficial effect of Nec-1 (*i.c.v.* 60μg) given just after surgery which was evidenced by attenuation of oligodendrocyte cell damage, diminution of APP (amyloid precursor protein) level, and protection of axons and myelin in the brain stem 2–6 days after injury. Moreover, Nec-1 administration resulted in a significant decrease in the BNIP3-positive oligodendrocytes suggesting an involvement of mitochondrial mechanisms in myelin protection mediated by Nec-1 (Mu et al. 2021).

Regarding the protective potential of Nec-1 in SCI, the first study was conducted by Wang et al. (2014a). In the rat SCI model (mechanical injury), Nec-1 given intrathecally (*i.t.* 1–50μg) 20 min before injury and 12–24 h after SCI in a dose-dependent manner attenuated the extent of lesion. Moreover, Nec-1 mitigated cell death (TUNEL-positive cells), reduced necroptotic (RIP1, RIP3 and MLKL) and

apoptotic (caspase-3, Bax/Bcl-2) markers, regulated oxidative stress parameters (ROS, MDA, and SOD), and inhibited release of pro-inflammatory cytokines (TNFα, IL1β, and IL-6). Moreover, it alleviated pathological changes and improved blood supply in the spinal cord trauma which was observed up to 7 weeks after injury (Wang et al. 2014a). In the next study in the same SCI model, it was evidenced that Nec-1 improved mitochondrial functions as observed 12–24 h after injury. Nec-1 reduced the elevated mitochondrial Ca^{2+}, preserved the decreased MMP, increased ATP production, promoted the activity of mitochondrial complex I, inhibited cytochrome c release, maintained the normal mitochondrial ultrastructure, increased mitochondrial biogenesis (Tfam, cytochrome b), and regulated their fusion (Mnf1, Mnf2) and fission (Fis1) (Wang et al. 2015). The next study explored the relationship between necroptosis and ER stress. The authors revealed that Nec-1 pretreatment reduced ultrastructural damage to the neuronal and astrocyte ER and mitochondria and inhibited neuronal expression of ER stress-related genes and proteins (Grp78, CHOP, XBP1) (Wang et al. 2017). In the SCI model (a laminectomy at T9 and compression with a vascular clip) in female mice, Nec-1 (*i.t.* 4μl of 4 mM) given 5 min after injury decreased PI-positive cell counts, alleviated tissue damage, increased the number of surviving neurons, and improved long-term functional recovery (Liu et al. 2015). However, Nec-1 did not show antiapoptotic properties (no changes in TUNEL-positive cells and in caspase-3), which is in contrast to observations made in the rat SCI model (Wang et al. 2014a). These discrepancies could be probably due to different Nec-1 doses, animal sexes, or species used in particular experiments. Another study performed in male mice showed that microglia/macrophages played a key role in inflammation after SCI and these immune cells were eliminated by necroptosis (Fan et al. 2015). Nec-1 given after injury and 2x/day for 5 days (*i.v.* 7.8 mg/kg) decreased the number of PI-positive microglia cells at day 5. Moreover, it was demonstrated that ER was involved in necroptosis of microglia/macrophages as measured by double and triple staining with cell-specific (Iba1 or CXCR4), necroptotic (MLKL), and ER stress (GRP78) markers (Fan et al. 2015). Finally, the beneficial effects of Nec-1 were confirmed in female mice where Nec-1 (*i.p.* 5 mg/kg) administered immediately after SCI and continued for a longer period of time (7–28 days) improved locomotor function and reduced spinal cord edema at day 7. These effects were associated with reduced RIP1, pRIP3, ROS, MDA, and increased level of ATP, MMP, SOD, and GSH observed at day 7 after SCI (Wang et al. 2019a) Interestingly, similar protective efficacy and mechanisms of action (apart from the influence on RIP1) were found for the RIP3 inhibitor GSK'872 (*i.p.* 2 mg/kg) (Wang et al. 2019a). Thus, results of the experimental studies strongly suggest that Nec-1 may have therapeutic potential for patients with acute brain or spinal cord injuries.

3.5 Retina Injuries

The retina is one of the most intensively studied parts of the CNS first of all to understand common blinding diseases (e.g., age-related macular degeneration,

glaucoma, anterior ischemic optic neuropathy, and diabetic retinopathy traumatic optic neuropathy) and also as a convenient model for examination of neurodegeneration induced by detrimental physical and ischemic factors. The first study investigating whether necroptosis contributes to retinal neuronal damage and functional impairment was carried out by Rosenbaum et al. (2010) in the rat model of retinal ischemia. They found that animals subjected to raised intraocular pressure for 45 min and receiving intravitreal injections of Nec-1 (2μl of 4 mM) during and 2 h after I/R showed a significant preservation in thickness and histoarchitecture of the inner retina and functional improvement compared with vehicle-treated controls, as observed 7 days post-injury. Its short-term effect (2–6 h) was connected with the inhibited autophagy (LC3) and decreased number of PI-positive but not TUNEL- or caspase-3-positive cells. Nec-1i serving as negative control was not protective in this study suggesting RIP1-dependent effects of Nec-1 in this model (Rosenbaum et al. 2010). These data were confirmed by the next study employing the mouse model of retinal I/R injury where Nec-1 (*i.p.* 2μg/g, 1 h before and continued once daily up to day 7) significantly improved neuronal cell survival in the ganglion cell layer. This effect was accompanied with attenuation of expression of proinflammatory genes (*Tnf, Il1b, Cybb, Nos2, Ccl2, Ccl5, Cxcl10, Icam1*) (Dvoriantchikova et al. 2014). Additionally, Kim et al. (2017) provided evidence that TNFα produced by astrocytes early after retinal I/R was responsible for necroptotic cell death of RGCs and showed that Nec-1 given intrevitreally (2μl of 0.1μg/ml) just after I/R via decreased RIP1 activation and improved the retina histopathology at all its layers. Finally, Do et al. (2017) showed that also another RIP1 inhibitor RIC (*i.p.* 10 and 30 mg/kg, given immediately after ischemia induction) was protective in the rat retina I/R model by increasing neuronal survival and attenuation of TUNEL-positive cell count in ganglion cell layer as found 3 days after I/R. Interestingly, RIC was also protective in retinal epithelial cell damage induced by single *i.p.* injection of 50 mg/kg of sodium iodate which models the pathogenesis of dry age-related macular degeneration. In this model, RIC administrated in a single dose (i.p. 20–30 mg/kg) or repeated doses (i.p. 330μg/ml, twice daily for 10 days starting at 3 days before injury) in eye drops prevented RPE loss and preserved retinal morphology without evoking cytotoxicity suggesting its putative clinical efficacy (Jang et al. 2019).

The induction of necroptosis was also observed in physical models of retina damage. Trichonas et al. (2010) was the first to demonstrate the protection of Nec-1 in the retinal detachment (RD) model. Although they showed in mice an increase in expression of RIP3 3–5 days after RD, intraretinal (*i.r.*) administration of Nec-1 (200μM) at the time of surgery was not protective. However, when it was combined with the apoptosis inhibitor, z-VAD-fmk, a partial prevention of photoreceptor loss was observed 3 days after injury as evidenced by the decreased number of TUNEL-positive cells, increased outer nuclear layer (ONL) thickness, reduced oxidative stress, prevented AIF translocation, and attenuated number of CD11-positive microglia/macrophages (Trichonas et al. 2010). In the next study, Dong et al. (2012) showed the protective effects of pre- and post-(6 h) treatment with Nec-1 (*i.r.* 400μM) but not with Nec-1i in the rat RD model as demonstrated by the improved photoreceptor survival and functional outcome. It was associated with the inhibition

of necroptotic (pRIP1, PI-positive cells) but not apoptotic processes (Dong et al. 2012). In the next study of those authors using the same experimental model, they additionally showed an involvement of autophagy inhibition in Nec-1-mediated photoreceptor protection as confirmed by ameliorated LC3II expression and autophagosome count (Dong et al. 2014). Necroptosis has been reported to be the major cell death pathway also in degenerating rod photoreceptors. In the P23H rhodopsin mutant rats and mice, a model representing one of the most common forms of retinal degeneration, upregulation of RIP1, RIP3 and activation of microglia and inflammasome (NLRP3/caspase-1/IL-1β) were found in P45 and/or P120 animals. In this genetic model of retinal degeneration, subcutaneous injection of Nec-1 s (15 mg/kg) once daily starting from P21 significantly preserved retina morphology and function which were superior to the effect mediated by antioxidant NAC (150 mg/kg). This protective effect of Nec-1 s was associated with inhibition of RIP1, RIP3, NFκB, ROS, DNA fragmentation, microglia activation, and inflammasome induction (Viringipurampeer et al., 2016). Nec-1 s was also tested in traumatic optic neuropathy induced by a blunt ocular injury in rats (Thomas et al. 2019). An intravitreal injection of Nec-1 s (5μl of 3.6 mM) just after injury and at 7 day did not improve histological and functional parameters evaluated at day 14. However, it prevented RGC loss at the center of the impact site as well as improved RGCs survival in primary cultures (Thomas et al. 2019). The presented data on Nec-1-mediated protection in various animal models of retina damage support further studies on the development of more clinically relevant RIP1 inhibitors for the of acute and chronic retinal pathologies.

3.6 Neurodegenerative Diseases

3.6.1 Alzheimer's Disease

In AD, neuronal degeneration in specific brain areas causes a dysfunction in learning and memory processes, and the pathology is associated with extracellular aggregation of amyloid-β (Aβ) and intarcellular hyperphosphorylation of tau. Apart from apoptotic processes, also necroptosis has been evidenced to be involved in the pathogenesis of AD (Caccamo et al. 2017), however there are rather limited in vivo studies on the effectiveness of Nec-1 in AD. In the study on APP/PS1 double transgenic mice, Nec-1 (*i.p.* 6.25 mg/kg, twice a week) given to 4-month-old animals and continued twice a week to 7 months (7 weeks of administration) significantly improved working spatial memory of the mutants which achieved the performance level observed in wild-type animals (Yang et al. 2017b). Moreover, Nec-1 reduced cortical and hippocampal level of β-amyloid (Aβ) oligomers, plaques, hyperphosphorylated tau, and tau aggregation without affecting Aβ production. These promising prophylactic effects of Nec-1 at the behavioral level were also demonstrated in the model of acutely induced memory deficits in ICR mice. Nec-1 (*i.v.* 6.25 mg/kg) given twice a week, starting a week before *i.c.v.* Aβ(1–42) injection and continued for the next week, significantly ameliorated memory deficits and histopathological features in these animals (Yang et al. 2017b). Further study using APP/PS1

double transgenic mice showed that Nec-1 also reduced necroptotic and apoptotic markers in the cortex of aged mutant mice (4 weeks treatment from 8 to 9 months) by decreasing the levels of p-RIP3 and Bax and increasing the levels of Bcl-2 (Yang et al. 2019b).

In chemical AD-like mouse model induced by a single *i.c.v.* aluminum administration ($AlCl_3$. 2μl of 2 mM), co-treatment with Nec-1 (*i.c.v.* 2μl of 4–8 mM) significantly improved learning and memory (Morris water maze task) and decreased the extent of neuronal cell damage in the hippocampal CA3 region observed 20 days after injection of the compounds. Moreover, Nec-1 reduced necrotic (pRIP1), apoptotic (caspase-3), autophagy (LC3II), and AD-related (Aβ and tau) proteins. However, when Nec-1 was given post-Al exposure (2–8 h) no protective effects were found (Qinli et al. 2013). These protective effects of Nec-1 were also confirmed in the chronic Al-based model (0.5% $AlCl_3$ given for 5 days). It was found that Nec-1 reduced Al-induced learning and memory impairment and decreased Al-evoked neuronal cell damage as measured 14 days after the last injections. Moreover, Nec-1 attenuated Al-induced changes in RIP1, caspase-3, and LC3II. The neuroprotective effect of Nec-1 was stronger than that mediated by the caspase inhibitor z-VAD-fmk, and combination of them resulted in synergistic action (Hao et al. 2020).

The factors indirectly linked with mild cognitive impairment and development of AD include neuroinflammation and diabetes. In the model of spatial memory impairment in rats induced by neuroinflammation (*i.c.v.* LPS 15μg), co-treatment with Nec-1 (*i.c.v.* 1μl 10μM) attenuated cognitive deficits measured by spontaneous alternations in the Y-maze test. This effect was associated with the reduced level of necroptosis (RIP1, RIP3), apoptosis (Bax/Bcl2, caspase-8, and caspase-3), oxidative stress (MDA), and increased antioxidant enzymes (SOD, GSH, and catalase) in the hippocampus and frontal cortex (Nikseresht et al. 2015). In the rat model of prediabetes (20 weeks of high-fat diet, HFD) which is characterized by cognitive decline and brain pathology, Nec-1 given from week 13 (s.c. 1.65 mg/kg/day) improved cognitive function, synaptic plasticity, and brain mitochondrial function and reduced hyperphosphorylated Tau. Moreover, it attenuated HFD-induced necroptosis (pRIP1, RIP3), oxidative stress, and microglia without alteration in insulin sensitivity (Jinawong et al. 2020). It has been shown that Nec-1 could be also beneficial in improving cognitive performance in the aged animals. Duan et al. (2018) using the accelerating aging mouse model induced by D-galactose (*i.p.* 25 mg/kg), administrated for 2 months and subjected to anesthesia and partial hepatectomy, demonstrated that Nec-1 (*i.p.* 6.25 mg/ml) given 1 h before surgery strikingly mitigated cognitive impairment and prevented neuronal loss and microglia activation in the DG hippocampal region. These effects were accompanied with decreased RIP1 level, improved synaptic plasticity (increase in Glu1A expression), and alleviated neuroinflammation (IL-1α, IL-1β, and TNFα) (Duan et al. 2018). All the above studies performed in various AD-like animal models provide substantial evidence that Nec-1 and its analogues could be promising candidates for the development of a neuroprotective drug for mild cognitive impairment (MCI) and AD.

3.6.2 Parkinson's Disease

The most significant pathological feature of PD is the progressive loss of dopaminergic neurons in the pars compacta of the substantia nigra (SNpc). In addition, PD has been also associated to neurodegeneration of other neuronal cell types including olfactory, cortical, and autonomic peripheral neurons. All these processes contribute to motor, cognitive, psychiatric, and peripheral symptoms in this chorea. Mitochondrial dysfunction and increased ROS level are thought to be the main causes of neuronal death in PD (Oñate et al., 2020). Only a few studies are available on the neuroprotective effects of Nec-1 or its stable analogue Nec-1 s in animal PD models. In the study by Iannielli et al. (2018) mice were injected daily with MPTP (*i.p.* 20 mg/kg; *1-methyl-4-phenyl-1,2,3,6-tetrahydropyridine*) for five consecutive days, while Nec-1 (*i.c.v.* 1μg/day) or Nec-1 s (*i.p.* 10 mg/kg/day) administration started 3 days after the first injection of MPTP and was continued for 3 weeks. Histological and biochemical analysis performed on day 24 showed comparable protective effects of both compounds evidenced by increased number of TH-positive neurons (by about 27%, the unbiased stereological sampling method) in the substantia nigra pars compacta (SNpc) and increased TH immunolabeling in DA striatal fibers (15% recovery, optical densitometry) when compared to the MPTP group. Moreover, Nec-1 s reduced intracellular oxidative stress level induced by MPTP injections as confirmed by immunohistochemistry for 4-hydroxynonenal (4-HNE) in TH + -nigral DA neurons (Iannielli et al., 2018). However, in another study employing the mouse MPTP model, Nec-1 s treatment (*i.p.* 10 mg/kg/day) initiated 1 h after a single MPTP (*i.p.* 40 mg/kg) injection and continued for the next 30 days was not protective, however, some tendency toward the increase in TH+ densitometry in SNpc could be noticed (Dionísio et al., 2019). It is not excluded that used various image analysis systems for calculation of TH+ cells in SNpc (quantitative vs. semiquantitative in Iannielli's and Dioniso's studies, respectively), animal numbers and/or different schedule of MPTP administration was responsible for the lack of a significant protection by Nec-1 s in the latter study. Nevertheless, these investigators reported that MPTP-induced dopaminergic neurodegeneration in the SNpc was attenuated in RIP3 knockout mice as compared with the wild-type mice (Dionísio et al. 2019). Lin et al. (2020) also used the mouse MPTP model to study the mechanisms of necroptosis and the effects of Nec-1. The used acute intoxication model involving the cumulative MPTP (*i.p.* 20 mg/kg) administration every 2 h up to 8 h (5 doses) led to the increased expression of necroptosis-related proteins (RIP1, RIP3, and MLKL), which were associated with DA neuronal loss in the SNpc. Treatment with Nec-1 (*i.p.* 1.65 mg/kg/day) initiated 12 h before application of MPTP and continued up to 21 days ameliorated DA neuronal loss in the SNpc (unbiased stereology of TH-positive neurons) and increased striatal DA level. The similar protective effects against MPTP were observed in RIP3−/− and MLKL−/− mice when compared to the wild-type ones where also the decreased level of pro-inflammatory cytokines (TNFα, IL-1β, and IL-6) was found suggesting the interplay between necroptosis and neuroinflammation in this PD model (Lin et al. 2020). Oñate et al. (2020) showed an induction of necroptosis (RIP3 and MLKL) in postmortem brain tissue from PD patients and in the 6-OHDA (*6-hydroxydopamine*)

PD model (4μg/μl, single injection to right striatum) in mice. Genetic ablation of necroptosis mediators (MLKL−/− and RIP3 −/− mice) as well as pharmacological inhibition of RIP1 by Nec-1 s (*i.p.* 8 mg/kg/day, 3 days before and 7 days after surgery) decreased DA neuronal loss in the SNpc, prevented striatal denervation, attenuated axonal loss, and improved animals motor performance. Finally, it has been shown that in mice treated with MPTP (*i.p.* 30 mg/kg for 5 days) there was an increase in necroptosis in TH-positive SNpc neurons which negatively correlated with expression of miR-425. Further molecular evaluation identified RIP1 as miR-425 target and intracerebral administration of miR-425 mimics (AgomiR-425) attenuated necroptosis activation and dopaminergic neuron loss as well as improved motor performance after MPTP administration in mice (Hu et al. 2019). All these results highlight the potential neuroprotective utility of Nec-1 or its analogues in preventing PD progression.

3.6.3 ALS and Other Neuropathies

Some data from preclinical studies and also clinical observations have suggested that necroptosis is involved in the pathogenesis of ALS (Re et al. 2014). Promising studies performed by Ito et al. (2016) using optineurin knockout mice (OPTN−/−) and SOD1(G93A) transgenic mice showed that axonal degeneration which preceded motor neuron loss was correlated with the activation of RIP1and RIP3. Similar observations were made in samples from human ALS patients suggesting necroptosis as a central player in progressive axonal degeneration. In 3 months-old OPTN−/− mice, Nec-1 s (oral dosing, 2.5–5 mg/day, for 1 month starting from 8 weeks of age) blocked demyelination in the spinal cord, prevented axonal loss and swelling, reduced the number of TUNEL-positive cells in the lumbar spinal cord, and improved motor performance in these animals. Similar protective effects of Nec-1 s were observed in SOD1(G93A) mice where additionally the RIP1 inhibitor delayed the onset of motor dysfunctions (Ito et al. 2016). However, recently the role of necroptosis in ALS was questioned. Dermentzaki et al. (2019) showed that constitutive deletion of RIP3 in SOD1(G93A) transgenic mice did not improve behavioral or neuropathological deficits. Moreover, no protection on myelin damage has been found in RIP3-silenced SOD1(G93A) and OPTN−/− mice. In addition, Wang et al. (2020) using SOD1(G93A) mice did not observe any beneficial effect of MLKL genetic ablation on disease onset, progression, and survival suggesting that motor neuron degeneration and activation of neuroinflammatory cells (astrocytes and microglia) are independent of MLKL expression. Moreover, while RIP1 accumulation occurred in the spinal cord of SOD1G93A mice in late-stage disease, RIP3 and MLKL expression levels were undetectable which is in contrast to results obtained by Ito et al. (2016). Thus, more preclinical investigations preferably using other models of ALS are needed to determine if necroptosis plays a critical role in the pathogenesis of ALS.

Necroptosis has been shown to be involved in various peripheral nerve injuries. Liang et al. (2019) found that in a rat sciatic nerve chronic constriction injury model there was a time-dependent increase in necroptosis-related proteins (RIP1 and RIP3) in the spinal cord which correlated well with the changes in mechanical and thermal

allodynia observed from day 1 to 21 after surgery. Nec-1 (*i.p.* 200–400μg/kg/day for 21 days) reduced peripheral nerve injury–related behavioral symptoms and it was associated with attenuation of necroptosis (RIP1, RIP3), reduction in the number of PI-positive cells, inhibition of NFκB activity, and decreased level of pro-inflammatory cytokines (TNFα, IL-1β, and substance P) (Liang et al. 2019). In the model of auditory neuropathy induced by ouabain, Wang et al. (2014b) observed the activation of necroptotic cell damage of the spiral ganglion cells (SGCs) which led to hearing loss. Nec-1 (10μl of 3 mM) given 10 min after ouabain (10μl of 10 mM) partially decreased SGC loss of the cochlear axis which was associated with reduction in RIP3 expression but it did not prevent hearing loss. However, a synergistic effect was observed when Nec-1 was combined with z-VAD-fmk (10μl of 3 mM) which led to almost complete inhibition of SGC death and significantly improved hearing function (Wang et al. 2014b). In their next study, using a similar model of auditory neuropathy, RIP3 ablation protected rats from ouabain-induced hearing damage and loss of function, while overexpression of RIP3 enhanced ouabain-induced injury that could be partially reversed by Nec-1. It was suggested that targeting RIP3 might prevent SGC death in clinical practice, and eventually might be helpful in the treatment of sensorineural hearing loss (Wang et al. 2021). Finally, in ex vivo model of mechanical sciatic and optic nerve injury, Nec-1 (100μM) given at the time of injury strongly delayed axonal degeneration after transection and also preserved their electrophysiological activity. It was associated with reduction in axonal mitochondrial fragmentation, and the inhibitor of mitochondrial fission Mdivi was protective in the model with similar efficacy as Nec-1 (Arrázola et al., 2019). Altogether, these results clearly support the potential clinical utility of Nec-1 and its derivatives in the treatment of various neuropathies.

3.6.4 Other Neurodegenerative Diseases

Nec-1 was demonstrated to be beneficial in the genetic Huntington's disease (HD) model, R6/2 transgenic mice (Zhu et al. 2011). Nec-1 (*i.c.v.*) administrated in osmotic pumps from 5 weeks of age, at week 11 helped to maintain the body weight and motor functions and was observed to significantly delay the disease onset (21.5%) but had a modest effect on survival of mice. It was postulated that, since Nec-1 treatment may revert necroptosis to apoptosis, concomitant treatment with both apoptosis and necroptosis inhibitors might be more efficient in the treatment of HD disease than each of these inhibitors given alone (Zhu et al. 2011). Moreover, an effectiveness of Nec-1 was demonstrated in the animal model of Niemann-Pick disease, type C1 (NPC1) which is characterized by progressive neuronal dysfunction, including cerebellar ataxia and dementia (Cougnoux et al. 2016). Treatment of Npc1-mutant mice with Nec-1 (*i.p.* 90 and 180 mg/kg) given every second day starting from the third week of age for the next 4 weeks significantly delayed cerebellar Purkinje cell loss and progression of neurological symptoms and increased lifespan (by about 10–14 days). No effect in the measured parameters was found for Nec-1i suggesting the involvement of RIP1-dependent mechanism of Nec-1 action in this genetic model of cerebral neurodegeneration (Cougnoux et al. 2016). Nec-1 was also considered for putative treatment of multiple sclerosis (MS).

In experimental autoimmune encephalomyelitis (EAE), a mouse model of MS, Nec-1 after repeated intrathecal injection (1.65 mg/kg) from day 2 every 3 days for 15 days decreased the number of lesions and inflammatory cell infiltrates in the spinal cord tissues and attenuated production of pro-inflammatory cytokines (TNFα, IL-1β and INFγ) in the EAE mice. In addition, it increased pDrp1/Drp1 and reduced necroptotic (pMLKL/MLKL) and apoptotic (Bax/Bcl-2, Bim) markers in the spinal cord tissue of EAE mice (Wang et al. 2019b).

Summing up the paragraph dedicated to neurodegenerative diseases, it is worth mentioning that DNL104, a selective and brain-penetrant inhibitor of RIP1, is in clinical development for AD and ALS (I phase). It was tested in healthy volunteers to investigate its safety and tolerability, pharmacokinetic profile in plasma and cerebrospinal fluid, and pharmacodynamic effects of RIP1 inhibition in peripheral blood mononuclear cells. DNL104 was well tolerated in the single-ascending dose and during the dosing period of the multiple ascending group. However, post-treatment liver toxicity was observed in 37.5% of subjects in the latter group which was assessed to be drug related. The authors also demonstrated that DNL104 led to RIP1 kinase inhibition, and this was not associated with CNS toxicities which supports development of CNS-penetrant RIP1 inhibitors in the future (Grievink et al. 2020).

4 Conclusions

In a critical appraisal of Nec-1 as a putative neuroprotectant some pros and cons should be taken into account. There is a substantial body of evidence suggesting that necroptosis contributes to the mechanism of neuronal damage related to hypoxia-ischemia, traumatic CNS injury, neuropathies, and neurodegenerative diseases. However, this programmed nonapoptotic cell death appears to be biochemically and functionally linked with several alternative cell death signaling pathways, and the relationship between various death pathways is extremely complex. Furthermore, although RIP1 is the key element in the concept of necroptosis, some data suggest that it can be involved also in non-necroptotic cell damage. Indeed, it has been found that RIP1 and RIP3 not only mediate necroptosis but also are involved in apoptosis and inflammatory signaling. Nec-1 is a potent inhibitor of RIP1, and most of the experimental studies used this compound in order to gain evidence that necroptosis is involved in neuronal damage under study and that Nec-1 may be proposed as a novel neuroprotectant in humans. Indeed, Nec-1 and its analogues like Nec-1 s display in in vivo models moderate neuroprotective effects, which are statistically significant, but rarely robust enough to be enthusiastic about them. In other words, Nec-1 when given alone failed to provide full neuroprotection in most tested experimental models and is more efficient in pre-treatment than in the clinically more desired post-treatment schedule. Some encouraging results have been obtained when Nec-1 was used in combination with an antiapoptotic agent, and this strategy appears to be more promising at least in some models on neuronal cell injury. Surprisingly, some neuroprotective effects of Nec-1 have been ascribed to

the inhibition of apoptosis, instead of necroptosis. Some other shortcomings of this compound as a candidate for a neuroprotective medicine have to be mentioned. Regarding physical properties and pharmacokinetics, its solubility in water is limited (requires DMSO) and after systemic administration its half-time is short. Although *i.c.v.* or intrathecal administration of Nec-1 attenuated neuronal damage to various extent in some experimental animal models, it is a hardly acceptable route of drug administration to patients. While remaining a highly valuable experimental tool in untangling the complex relationships between various signaling neuronal death pathways and elucidating molecular mechanism of CNS pathologies, it is rather not likely to be considered a candidate for a neuroprotective drug. Further development of novel necroptosis inhibitors with more favorable pharmacokinetic characteristics, therapeutic efficacy, and safety profiles is required.

5 Cross-References

- ▶ 6-Hydroxydopamine Lesioning of Dopamine Neurons in Neonatal and Adult Rats Induces Age-Dependent Consequences
- ▶ Aluminum and Neurodegenerative Disease
- ▶ Excitotoxicity and Amyotrophic Lateral Sclerosis
- ▶ Glutamate and Neurodegeneration in the Retina
- ▶ Huntington's Disease and Neurodegeneration
- ▶ Iron Neurotoxicity in Parkinson's Disease
- ▶ MPTP Neurotoxicity: Actions, Mechanisms, and Animal Modeling of Parkinson's Disease
- ▶ Neurotoxicity and ALS: Insights into Pathogenesis
- ▶ Neurotoxicity in Huntington Disease
- ▶ Pathogenesis of Alzheimer's Disease

References

Arrázola, M. S., Saquel, C., Catalán, R. J., Barrientos, S. A., Hernandez, D. E., Martínez, N. W., Catenaccio, A., & Court, F. A. (2019). Axonal degeneration is mediated by necroptosis activation. *The Journal of Neuroscience, 39*, 3832–3844.

Askalan, R., Gabarin, N., Armstrong, E. A., Fang, L. Y., Couchman, D., & Yager, J. Y. (2015). Mechanisms of neurodegeneration after severe hypoxic-ischemic injury in the neonatal rat brain. *Brain Research, 1629*, 94–103.

Bao, Z., Fan, L., Zhao, L., Xu, X., Liu, Y., Chao, H., Liu, N., You, Y., Liu, Y., Wang, X., & Ji, J. (2019). Silencing of A20 aggravates neuronal death and inflammation after traumatic brain injury: A potential trigger of necroptosis. *Frontiers in Molecular Neuroscience, 12*, 222.

Caccamo, A., Branca, C., Piras, I. S., Ferreira, E., Huentelman, M. J., Liang, W. S., Readhead, B., Dudley, J. T., Spangenberg, E. E., Green, K. N., Belfiore, R., Winslow, W., & Oddo, S. (2017). Necroptosis activation in Alzheimer's disease. *Nature Neuroscience, 20*, 1236–1246.

Cao, L., & Mu, W. (2020). Necrostatin-1 and necroptosis inhibition: Pathophysiology and therapeutic implications. *Pharmacological Research, 163*, 105297.

Chang, P., Dong, W., Zhang, M., Wang, Z., Wang, Y., Wang, T., Gao, Y., Meng, H., Luo, B., Luo, C., Chen, X., & Tao, L. (2014). Anti-necroptosis chemical necrostatin-1 can also suppress apoptotic and autophagic pathway to exert neuroprotective effect in mice intracerebral hemorrhage model. *Journal of Molecular Neuroscience, 52*, 242–249.

Chavez-Valdez, R., Flock, D. L., Martin, L. J., & Northington, F. J. (2016). Endoplasmic reticulum pathology and stress response in neurons precede programmed necrosis after neonatal hypoxia-ischemia. *International Journal of Developmental Neuroscience, 48*, 58–70.

Chavez-Valdez, R., Martin, L. J., Flock, D. L., & Northington, F. J. (2012). Necrostatin-1 attenuates mitochondrial dysfunction in neurons and astrocytes following neonatal hypoxia-ischemia. *Neuroscience, 219*, 192–203.

Chavez-Valdez, R., Martin, L. J., Razdan, S., Gauda, E. B., & Northington, F. J. (2014). Sexual dimorphism in BDNF signaling after neonatal hypoxia-ischemia and treatment with necrostatin-1. *Neuroscience, 260*, 106–119.

Chen, F., Su, X., Lin, Z., Lin, Y., Yu, L., Cai, J., Kang, D., & Hu, L. (2017). Necrostatin-1 attenuates early brain injury after subarachnoid hemorrhage in rats by inhibiting necroptosis. *Neuropsychiatric Disease and Treatment, 13*, 1771–1782.

Chen, J., Jin, H., Xu, H., Peng, Y., Jie, L., Xu, D., Chen, L., Li, T., Fan, L., He, P., Ying, G., Gu, C., Wang, C., Wang, L., & Chen, G. (2019). The neuroprotective effects of necrostatin-1 on subarachnoid hemorrhage in rats are possibly mediated by preventing blood-brain barrier disruption and RIP3-mediated necroptosis. *Cell Transplantation, 28*, 1358–1372.

Chen, Y., Zhang, L., Yu, H., Song, K., Shi, J., Chen, L., & Cheng, J. (2018). Necrostatin-1 improves long-term functional recovery through protecting oligodendrocyte precursor cells after transient focal cerebral ischemia in mice. *Neuroscience, 2018*(371), 229–241.

Conrad, M., Angeli, J. P., Vandenabeele, P., & Stockwell, B. R. (2016). Regulated necrosis: Disease relevance and therapeutic opportunities. *Nature Reviews. Drug Discovery, 15*, 348–366.

Cougnoux, A., Cluzeau, C., Mitra, S., Li, R., Williams, I., Burkert, K., Xu, X., Wassif, C. A., Zheng, W., & Porter, F. D. (2016). Necroptosis in Niemann-Pick disease, type C1: A potential therapeutic target. *Cell Death & Disease, 7*, e2147.

Degterev, A., Hitomi, J., Germscheid, M., Ch'en, I. L., Korkina, O., Teng, X., Abbott, D., Cuny, G. D., Yuan, C., Wagner, G., Hedrick, S. M., Gerber, S. A., Lugovskoy, A., & Yuan, J. (2008). Identification of RIP1 kinase as a specific cellular target of necrostatins. *Nature Chemical Biology, 4*, 313–321.

Degterev, A., Huang, Z., Boyce, M., Li, Y., Jagtap, P., Mizushima, N., Cuny, G. D., Mitchison, T. J., Moskowitz, M. A., & Yuan, J. (2005). Chemical inhibitor of nonapoptotic cell death with therapeutic potential for ischemic brain injury. *Nature Chemical Biology, 1*, 112–119.

Degterev, A., Ofengeim, D., & Yuan, J. (2019). Targeting RIPK1 for the treatment of human diseases. *Proceedings of the National Academy of Sciences of the United States of America, 116*, 9714–9722.

Deng, X. X., Li, S. S., & Sun, F. Y. (2019). Necrostatin-1 prevents necroptosis in brains after ischemic stroke via inhibition of RIPK1-mediated RIPK3/MLKL signaling. *Aging and Disease, 10*, 807–817.

Dermentzaki, G., Politi, K.A., Lu, L., Mishra, V., Pérez-Torres, E.J., Sosunov, A.A., McKhann, G.M. 2nd., Lotti, F., Shneider, N.A., Przedborski, S. (2019). Deletion of Ripk3 prevents motor neuron death in vitro but not in vivo. *eNeuro, 6*(1), ENEURO.0308-18.2018.

Dionísio, P. A., Oliveira, S. R., Gaspar, M. M., Gama, M. J., Castro-Caldas, M., Amaral, J. D., & Rodrigues, C. M. P. (2019). Ablation of RIP3 protects from dopaminergic neurodegeneration in experimental Parkinson's disease. *Cell Death & Disease, 10*, 840.

Do, Y. J., Sul, J. W., Jang, K. H., Kang, N. S., Kim, Y. H., Kim, Y. G., & Kim, E. (2017). A novel RIPK1 inhibitor that prevents retinal degeneration in a rat glaucoma model. *Experimental Cell Research, 359*, 30–38.

Dong, K., Zhu, H., Song, Z., Gong, Y., Wang, F., Wang, W., Zheng, Z., Yu, Z., Gu, Q., Xu, X., & Sun, X. (2012). Necrostatin-1 protects photoreceptors from cell death and improves functional outcome after experimental retinal detachment. *The American Journal of Pathology, 181*, 1634–1641.

Dong, K., Zhu, Z. C., Wang, F. H., Ke, G. J., Yu, Z., & Xu, X. (2014). Activation of autophagy in photoreceptor necroptosis after experimental retinal detachment. *International Journal of Ophthalmology, 7*, 745–752.

Duan, S., Wang, X., Chen, G., Quan, C., Qu, S., & Tong, J. (2018). Inhibiting RIPK1 limits neuroinflammation and alleviates postoperative cognitive impairments in D-Galactose-induced aged mice. *Frontiers in Behavioral Neuroscience, 12*, 138.

Dvoriantchikova, G., Degterev, A., & Ivanov, D. (2014). Retinal ganglion cell (RGC) programmed necrosis contributes to ischemia-reperfusion-induced retinal damage. *Experimental Eye Research, 123*, 1–7.

Fan, H., Tang, H.-B., Kang, J., Shan, L., Song, H., Zhu, K., Wang, J., Ju, G., & Wang, Y.-Z. (2015). Involvement of endoplasmic reticulum stress in the necroptosis of microglia/macrophages after spinal cord injury. *Neuroscience, 311*, 362–373.

Fan, J., Dawson, T. M., & Dawson, V. L. (2017). Cell death mechanisms of neurodegeneration. *Advances in Neurobiology, 15*, 403–425.

Fang, Y., Gao, S., Wang, X., Cao, Y., Lu, J., Chen, S., Lenahan, C., Zhang, J. H., Shao, A., & Zhang, J. (2020). Programmed cell deaths and potential crosstalk with blood-brain barrier dysfunction after hemorrhagic stroke. *Frontiers in Cellular Neuroscience, 14*, 68.

Geng, F., Yin, H., Li, Z., Li, Q., He, C., Wang, Z., & Yu, J. (2017). Quantitative analysis of necrostatin-1, a necroptosis inhibitor by LC-MS/MS and the study of its pharmacokinetics and bioavailability. *Biomedicine & Pharmacotherapy, 95*, 1479–1485.

Grievink, H. W., Heuberger, J. A. A. C., Huang, F., Chaudhary, R., Birkhoff, W. A. J., Tonn, G. R., Mosesova, S., Erickson, R., Moerland, M., Haddick, P. C. G., Scearce-Levie, K., Ho, C., & Groeneveld, G. J. (2020). DNL104, a centrally penetrant RIPK1 inhibitor, inhibits RIP1 kinase phosphorylation in a randomized phase I ascending dose study in healthy volunteers. *Clinical Pharmacology and Therapeutics, 107*, 406–414.

Hao, Y. X., Li, M. Q., Zhang, J. S., Zhang, Q. L., Jiao, X., Ji, X. L., Li, H., & Niu, Q. (2020). Aluminum-induced "mixed" cell death in mice cerebral tissue and potential intervention. *Neurotoxicity Research, 37*, 835–846.

Hu, Y. B., Zhang, Y. F., Wang, H., Ren, R. J., Cui, H. L., Huang, W. Y., Cheng, Q., Chen, H. Z., & Wang, G. (2019). miR-425 deficiency promotes necroptosis and dopaminergic neurodegeneration in Parkinson's disease. *Cell Death & Disease, 10*, 589.

Iannielli, A., Bido, S., Folladori, L., Segnali, A., Cancellieri, C., Maresca, A., Massimino, L., Rubio, A., Morabito, G., Caporali, L., Tagliavini, F., Musumeci, O., Gregato, G., Bezard, E., Carelli, V., Tiranti, V., & Broccoli, V. (2018). Pharmacological inhibition of necroptosis protects from dopaminergic neuronal cell death in Parkinson's disease models. *Cell Reports, 22*, 2066–2079.

Ito, Y., Ofengeim, D., Najafov, A., Das, S., Saberi, S., Li, Y., Hitomi, J., Zhu, H., Chen, H., Mayo, L., Geng, J., Amin, P., DeWitt, J. P., Mookhtiar, A. K., Florez, M., Ouchida, A. T., Fan, J. B., Pasparakis, M., Kelliher, M. A., … Yuan, J. (2016). RIPK1 mediates axonal degeneration by promoting inflammation and necroptosis in ALS. *Science, 353*, 603–608.

Jang, K. H., Do, Y. J., Koo, T. S., Choi, J. S., Song, E. J., Hwang, Y., Bae, H. J., Lee, J. H., & Kim, E. (2019). Protective effect of RIPK1-inhibitory compound in in vivo models for retinal degenerative disease. *Experimental Eye Research, 180*, 8–17.

Jantas, D., Chwastek, J., Grygier, B., & Lasoń, W. (2020). Neuroprotective effects of Necrostatin-1 against oxidative stress-induced cell damage: An involvement of cathepsin D inhibition. *Neurotoxicity Research, 37*, 525–542.

Jiao, Y., Wang, J., Zhang, H., Cao, Y., Qu, Y., Huang, S., Kong, X., Song, C., Li, J., Li, Q., Ma, H., Lu, X., & Wang, L. (2020). Inhibition of microglial receptor-interacting protein kinase 1 ameliorates neuroinflammation following cerebral ischaemic stroke. *Journal of Cellular and Molecular Medicine, 24*, 12585–12598.

Jinawong, K., Apaijai, N., Wongsuchai, S., Pratchayasakul, W., Chattipakorn, N., & Chattipakorn, S. C. (2020). Necrostatin-1 mitigates cognitive dysfunction in prediabetic rats with no alteration in insulin sensitivity. *Diabetes, 69*, 1411–1423.

Kim, C. R., Kim, J. H., Park, H. L., & Park, C. K. (2017). Ischemia reperfusion injury triggers TNFα induced-necroptosis in rat retina. *Current Eye Research, 42*, 771–779.

King, M. D., Whitaker-Lea, W. A., Campbell, J. M., Alleyne, C. H., Jr., & Dhandapani, K. M. (2014). Necrostatin-1 reduces neurovascular injury after intracerebral hemorrhage. *International Journal of Cell Biology, 2014*, 495817.

Li, J., Zhang, J., Zhang, Y., Wang, Z., Song, Y., Wei, S., He, M., You, S., Jia, J., & Cheng, J. (2019). TRAF2 protects against cerebral ischemia-induced brain injury by suppressing necroptosis. *Cell Death & Disease, 10*, 328.

Li, W., Liu, J., Chen, J. R., Zhu, Y. M., Gao, X., Ni, Y., Lin, B., Li, H., Qiao, S. G., Wang, C., Zhang, H. L., & Ao, G. Z. (2018). Neuroprotective effects of DTIO, a novel analogue of Nec-1, in acute and chronic stages after ischemic stroke. *Neuroscience, 390*, 12–29.

Liang, Y. X., Wang, N. N., Zhang, Z. Y., Juan, Z. D., & Zhang, C. (2019). Necrostatin-1 ameliorates peripheral nerve injury-induced neuropathic pain by inhibiting the RIP1/RIP3 pathway. *Frontiers in Cellular Neuroscience, 13*, 211.

Lin, Q. S., Chen, P., Wang, W. X., Lin, C. C., Zhou, Y., Yu, L. H., Lin, Y. X., Xu, Y. F., & Kang, D. Z. (2020). RIP1/RIP3/MLKL mediates dopaminergic neuron necroptosis in a mouse model of Parkinson disease. *Laboratory Investigation, 100*, 503–511.

Liu, M., Wu, W., Li, H., Li, S., Huang, L. T., Yang, Y. Q., Sun, Q., Wang, C. X., Yu, Z., & Hang, C. H. (2015). Necroptosis, a novel type of programmed cell death, contributes to early neural cells damage after spinal cord injury in adult mice. *The Journal of Spinal Cord Medicine, 38*, 745–753.

Mehta, S. L., Manhas, N., & Raghubir, R. (2007). Molecular targets in cerebral ischemia for developing novel therapeutics. *Brain Research Reviews, 54*, 34–66.

Mikuš, P., Pecher, D., Rauová, D., Horváth, C., Szobi, A., & Adameová, A. (2018). Determination of novel highly effective necrostatin Nec-1s in rat plasma by high performance liquid chromatography hyphenated with quadrupole-time-of-flight mass spectrometry. *Molecules, 23*, 1946.

Mu, J., Weng, J., Yang, C., Guan, T., Deng, L., Li, M., Zhang, G., & Kong, J. (2021). Necrostatin-1 prevents the proapoptotic protein Bcl-2/adenovirus E1B 19-kDa interacting protein 3 from integration into mitochondria. *Journal of Neurochemistry, 156*, 929–942.

Ni, Y., Gu, W. W., Liu, Z. H., Zhu, Y. M., Rong, J. G., Kent, T. A., Li, M., Qiao, S. G., An, J. Z., & Zhang, H. L. (2018). RIP1K contributes to neuronal and astrocytic cell death in ischemic stroke via activating autophagic-lysosomal pathway. *Neuroscience, 371*, 60–74.

Nikseresht, S., Khodagholi, F., & Ahmadiani, A. (2019). Protective effects of ex-527 on cerebral ischemia-reperfusion injury through necroptosis signaling pathway attenuation. *Journal of Cellular Physiology, 234*, 1816–1826.

Nikseresht, S., Khodagholi, F., Nategh, M., & Dargahi, L. (2015). RIP1 inhibition rescues from Lps-induced Rip3-mediated programmed cell death, distributed energy metabolism and spatial memory impairment. *Journal of Molecular Neuroscience, 57*, 219–230.

Northington, F. J., Chavez-Valdez, R., Graham, E. M., Razdan, S., Gauda, E. B., & Martin, L. J. (2011). Necrostatin decreases oxidative damage, inflammation, and injury after neonatal HI. *Journal of Cerebral Blood Flow and Metabolism, 31*, 178–189.

Oñate, M., Catenaccio, A., Salvadores, N., Saquel, C., Martinez, A., Moreno-Gonzalez, I., Gamez, N., Soto, P., Soto, C., Hetz, C., & Court, F. A. (2020). The necroptosis machinery mediates axonal degeneration in a model of Parkinson disease. *Cell Death and Differentiation, 27*, 1169–1185.

Qinli, Z., Meiqing, L., Xia, J., Li, X., Weili, G., Xiuliang, J., Junwei, J., Hailan, Y., Ce, Z., & Qiao, N. (2013). Necrostatin-1 inhibits the degeneration of neural cells induced by aluminum exposure. *Restorative Neurology and Neuroscience, 31*, 543–555.

Re, D. B., Le Verche, V., Yu, C., Amoroso, M. W., Politi, K. A., Phani, S., Ikiz, B., Hoffmann, L., Koolen, M., Nagata, T., Papadimitriou, D., Nagy, P., Mitsumoto, H., Kariya, S., Wichterle, H., Henderson, C. E., & Przedborski, S. (2014). Necroptosis drives motor neuron death in models of both sporadic and familial ALS. *Neuron, 81*, 1001–1008.

Rosenbaum, D. M., Degterev, A., David, J., Rosenbaum, P. S., Roth, S., Grotta, J. C., Cuny, G. D., Yuan, J., & Savitz, S. I. (2010). Necroptosis, a novel form of caspase-independent cell death, contributes to neuronal damage in a retinal ischemia-reperfusion injury model. *Journal of Neuroscience Research, 88*, 1569–1576.

Savard, A., Brochu, M. E., Chevin, M., Guiraut, C., Grbic, D., & Sébire, G. (2015). Neuronal self-injury mediated by IL-1β and MMP-9 in a cerebral palsy model of severe neonatal

encephalopathy induced by immune activation plus hypoxia-ischemia. *Journal of Neuroinflammation, 12*, 111.

Su, X., Wang, H., Kang, D., Zhu, J., Sun, Q., Li, T., & Ding, K. (2015). Necrostatin-1 ameliorates intracerebral hemorrhage-induced brain injury in mice through inhibiting RIP1/RIP3 pathway. *Neurochemical Research, 40*, 643–650.

Takahashi, N., Duprez, L., Grootjans, S., Cauwels, A., Nerinckx, W., DuHadaway, J. B., Goossens, V., Roelandt, R., Van Hauwermeiren, F., Libert, C., Declercq, W., Callewaert, N., Prendergast, G. C., Degterev, A., Yuan, J., & Vandenabeele, P. (2012). Necrostatin-1 analogues: Critical issues on the specificity, activity and in vivo use in experimental disease models. *Cell Death & Disease, 3*, e437.

Teng, X., Degterev, A., Jagtap, P., Xing, X., Choi, S., Denu, R., Yuan, J., & Cuny, G. D. (2005). Structure-activity relationship study of novel necroptosis inhibitors. *Bioorganic & Medicinal Chemistry Letters, 15*, 5039–5044.

Thomas, C. N., Thompson, A. M., Ahmed, Z., & Blanch, R. J. (2019). Retinal ganglion cells die by necroptotic mechanisms in a site-specific manner in a rat blunt ocular injury model. *Cell, 8*, 1517.

Trichonas, G., Murakami, Y., Thanos, A., Morizane, Y., Kayama, M., Debouck, C. M., Hisatomi, T., Miller, J. W., & Vavvas, D. G. (2010). Receptor interacting protein kinases mediate retinal detachment-induced photoreceptor necrosis and compensate for inhibition of apoptosis. *Proceedings of the National Academy of Sciences of the United States of America, 107*, 21695–21700.

Vanden Berghe, T., Kaiser, W. J., Bertrand, M. J., & Vandenabeele, P. (2015). Molecular crosstalk between apoptosis, necroptosis, and survival signaling. *Molecular & Cellular Oncology, 2*, e975093.

Vandenabeele, P., Galluzzim, L., Vanden Berghem, T., & Kroemer, G. (2010). Molecular mechanisms of necroptosis: An ordered cellular explosion. *Nature Reviews. Molecular Cell Biology, 11*, 700–714.

Viringipurampeer, I. A., Metcalfe, A. L., Bashar, A. E., Sivak, O., Yanai, A., Mohammadi, Z., Moritz, O. L., Gregory-Evans, C. Y., & Gregory-Evans, K. (2016). NLRP3 inflammasome activation drives bystander cone photoreceptor cell death in a P23H rhodopsin model of retinal degeneration. *Human Molecular Genetics, 25*, 1501–1516.

Wang, S., Wu, J., Zeng, Y. Z., Wu, S. S., Deng, G. R., Chen, Z. D., & Lin, B. (2017). Necrostatin-1 mitigates endoplasmic reticulum stress after spinal cord injury. *Neurochemical Research, 42*, 3548–3558.

Wang, T., Perera, N. D., Chiam, M. D. F., Cuic, B., Wanniarachchillage, N., Tomas, D., Samson, A. L., Cawthorne, W., Valor, E. N., Murphy, J. M., & Turner, B. J. (2020). Necroptosis is dispensable for motor neuron degeneration in a mouse model of ALS. *Cell Death and Differentiation, 27*, 1728–1739.

Wang, X., Mao, X., Liang, K., Chen, X., Yue, B., & Yang, Y. (2021). RIP3-mediated necroptosis was essential for spiral ganglion neuron damage. *Neuroscience Letters, 744*, 135565.

Wang, X., Wang, Y., Ding, Z. J., Yue, B., Zhang, P. Z., Chen, X. D., Chen, X., Chen, J., Chen, F. Q., Chen, Y., Wang, R. F., Mi, W. J., Lin, Y., Wang, J., & Qiu, J. H. (2014b). The role of RIP3 mediated necroptosis in ouabain-induced spiral ganglion neurons injuries. *Neuroscience Letters, 578*, 111–116.

Wang, Y., Guo, L., Wang, J., Shi, W., Xia, Z., & Li, B. (2019b). Necrostatin-1 ameliorates the pathogenesis of experimental autoimmune encephalomyelitis by suppressing apoptosis and necroptosis of oligodendrocyte precursor cells. *Experimental and Therapeutic Medicine, 18*, 4113–4119.

Wang, Y., Jiao, J., Zhang, S., Zheng, C., & Wu, M. (2019a). RIP3 inhibition protects locomotion function through ameliorating mitochondrial antioxidative capacity after spinal cord injury. *Biomedicine & Pharmacotherapy, 116*, 109019.

Wang, Y., Wang, H., Tao, Y., Zhang, S., Wang, J., & Feng, X. (2014a). Necroptosis inhibitor necrostatin-1 promotes cell protection and physiological function in traumatic spinal cord injury. *Neuroscience, 266*, 91–101.

Wang, Y., Wang, J., Yang, H., Zhou, J., Feng, X., Wang, H., & Tao, Y. (2015). Necrostatin-1 mitigates mitochondrial dysfunction post-spinal cord injury. *Neuroscience, 289*, 224–232.

Wang, Y. Q., Wang, L., Zhang, M. Y., Wang, T., Bao, H. J., Liu, W. L., Dai, D. K., Zhang, L., Chang, P., Dong, W. W., Chen, X. P., & Tao, L. Y. (2012). Necrostatin-1 suppresses autophagy and apoptosis in mice traumatic brain injury model. *Neurochemical Research, 37*, 1849–1858.

Xie, T., Peng, W., Liu, Y., Yan, C., Maki, J., Degterev, A., Yuan, J., & Shi, Y. (2013). Structural basis of RIP1 inhibition by necrostatins. *Structure, 21*, 493–499.

Xu, X., Chua, K. W., Chua, C. C., Liu, C. F., Hamdy, R. C., & Chua, B. H. (2010). Synergistic protective effects of humanin and necrostatin-1 on hypoxia and ischemia/reperfusion injury. *Brain Research, 1355*, 189–194.

Yang, C., Li, T., Xue, H., Wang, L., Deng, L., Xie, Y., Bai, X., Xin, D., Yuan, H., Qiu, J., Wang, Z., & Li, G. (2019a). Inhibition of necroptosis rescues SAH-induced synaptic impairments in hippocampus via CREB-BDNF pathway. *Frontiers in Neuroscience, 12*, 990.

Yang, R., Hu, K., Chen, J., Zhu, S., Li, L., Lu, H., Li, P., & Dong, R. (2017a). Necrostatin-1 protects hippocampal neurons against ischemia/reperfusion injury via the RIP3/DAXX signaling pathway in rats. *Neuroscience Letters, 651*, 207–215.

Yang, S. H., Lee, D. K., Shin, J., Lee, S., Baek, S., Kim, J., Jung, H., Hah, J. M., & Kim, Y. (2017b). Nec-1 alleviates cognitive impairment with reduction of Abeta and tau abnormalities in APP/PS1 mice. *EMBO Molecular Medicine, 9*, 61–77.

Yang, S. H., Shin, J., Shin, N. N., Hwang, J. H., Hong, S. C., Park, K., Lee, J. W., Lee, S., Baek, S., Kim, K., Cho, I., & Kim, Y. (2019b). A small molecule Nec-1 directly induces amyloid clearance in the brains of aged APP/PS1 mice. *Scientific Reports, 9*, 4183.

Yin, B., Xu, Y., Wei, R. L., He, F., Luo, B. Y., & Wang, J. Y. (2015). Inhibition of receptor-interacting protein 3 upregulation and nuclear translocation involved in Necrostatin-1 protection against hippocampal neuronal programmed necrosis induced by ischemia/reperfusion injury. *Brain Research, 1609*, 63–71.

You, Z., Savitz, S. I., Yang, J., Degterev, A., Yuan, J., Cuny, G. D., Moskowitz, M. A., & Whalen, M. J. (2008). Necrostatin-1 reduces histopathology and improves functional outcome after controlled cortical impact in mice. *Journal of Cerebral Blood Flow and Metabolism, 28*, 1564–1573.

Zhang, S., Tang, M. B., Luo, H. Y., Shi, C. H., & Xu, Y. M. (2017). Necroptosis in neurodegenerative diseases: A potential therapeutic target. *Cell Death & Disease, 8*, e2905.

Zhao, H., Jaffer, T., Eguchi, S., Wang, Z., Linkermann, A., & Ma, D. (2015). Role of necroptosis in the pathogenesis of solid organ injury. *Cell Death & Disease, 6*, e1975.

Zhou, K., Shi, L., Wang, Z., Zhou, J., Manaenko, A., Reis, C., Chen, S., & Zhang, J. (2017). RIP1-RIP3-DRP1 pathway regulates NLRP3 inflammasome activation following subarachnoid hemorrhage. *Experimental Neurology, 295*, 116–124.

Zhu, S., Zhang, Y., Bai, G., & Li, H. (2011). Necrostatin-1 ameliorates symptoms in R6/2 transgenic mouse model of Huntington's disease. *Cell Death & Disease, 2*, e115.

Zhu, X., Park, J., Golinski, J., Qiu, J., Khuman, J., Lee, C. C., Lo, E. H., Degterev, A., Whalen, M., & J. (2014). Role of Akt and mammalian target of rapamycin in functional outcome after concussive brain injury in mice. *Journal of Cerebral Blood Flow and Metabolism, 34*, 1531–1539.